

HIGH-VOLTAGE PROGRAMMABLE DELTA-SIGMA MODULATION
VOLTAGE-CONTROL CIRCUIT

by
Lucien Jan Bissey

A thesis
submitted in partial fulfillment
of the requirements for the degree of
Master of Science in Electrical Engineering
Boise State University

May 2010

BOISE STATE UNIVERSITY GRADUATE COLLEGE

DEFENSE COMMITTEE APPROVAL

of the thesis submitted by

Lucien Jan Bissey

We have read and discussed the thesis submitted by student Lucien Jan Bissey, and we have also evaluated his presentation and response to questions during the final oral examination. We find that the student has passed the final oral examination, and that the thesis is satisfactory for a master's degree and ready for any final modifications that we may explicitly require.

Date

R. Jacob Baker, Ph.D.
Chair, Supervisory Committee

Date

Kristy A. Campbell, Ph.D.
Member, Supervisory Committee

Date

Wan Kuang, Ph.D.
Member, Supervisory Committee

BOISE STATE UNIVERSITY GRADUATE COLLEGE

FINAL READING APPROVAL

of the thesis submitted by

Lucien Jan Bissey

To the Graduate College of Boise State University:

I have read the thesis of Lucien Jan Bissey in its final form and have found that (1) the modifications required by the defense committee are complete; (2) the format, citations, and bibliographic style are consistent and acceptable; (3) the illustrative materials including figures, tables, and charts are in place; and (4) the final manuscript is ready for submission to the Graduate College.

Date

R. Jacob Baker, Ph.D.
Chair, Supervisory Committee

Approved for the Graduate College:

Date

John R. Pelton, Ph.D.
Dean of the Graduate College

BOISE STATE UNIVERSITY GRADUATE COLLEGE

DEFENSE COMMITTEE AND FINAL READING APPROVALS

of the thesis submitted by

Lucien Jan Bissey

Thesis Title: High-Voltage Programmable Delta-Sigma Modulation Voltage Control Circuit

Date of Final Oral Examination: 05 April 2010

The following individuals read and discussed the thesis submitted by student Lucien Jan Bissey, and they also evaluated his presentation and response to questions during the final oral examination. They found that the student passed the final oral examination, and that the thesis was satisfactory for a master's degree and ready for any final modifications that they explicitly required.

R. Jacob Baker, Ph.D. Chair, Supervisory Committee

Kristy A. Campbell, Ph.D. Member, Supervisory Committee

Wan Kuang, Ph.D. Member, Supervisory Committee

The final reading approval of the thesis was granted by R. Jacob Baker, Ph.D., Chair of the Supervisory Committee. The thesis was approved for the Graduate College by John R. Pelton, Ph.D., Dean of the Graduate College.

DEDICATION

This thesis is dedicated to my family, and particularly my wife Michelle who has remained by my side throughout all of the trials encountered in an endeavor of this magnitude. Her encouragement and patience throughout all of my studies has kept me moving forward and this is the product of all our hard work.

ACKNOWLEDGEMENTS

I would like to take this opportunity to express my gratitude to Dr. Baker. He has been a significant source of education throughout my undergraduate and graduate experiences. His focus on the student and learning with practical application of the material has made a significant difference in my educational and professional life. The skills in the engineering field that I have absorbed from Dr. Baker have aided me in the past and will continue to serve me well throughout my career. At no time was it easy to understand the material to the degree that I desired, but Dr. Baker was there to challenge my knowledge and teach me different methods and ways to think about problem solving. The best experiences were solving difficult problems and experiencing the “Ah Ha” moments that inevitably arrive. It is in those moments that the true magnitude of my appreciation comes to light. I would refrain from calling him since it was usually in the middle of the night. I would also like to thank him for the many years of personal friendship that we have experienced.

I would also extend my appreciation to Micron Technology, specifically Kevin Duesman, for allowing me to pursue this goal and financing my educational pursuits. Without this funding and support this would have been significantly more difficult to achieve.

Finally, I would like to thank my wife Michelle. It is she who would tolerate my rants about how a simulation would not work. She would encourage me to sleep on

it and try again in the morning and then not question when the inspiration would occur at 2am and I would stagger out of bed to try one more time. It was Michelle who reminded me of my initial desire for a Masters Degree and to move forward and not surrender. Without her love, friendship, and patience I would have ceased this endeavor and gone fishing.

ABSTRACT

Modern memory semiconductors require different internal voltages to accomplish the myriad of tasks that are required for operation. These internal voltages are multiples of the external voltage that is applied to the part. This multiple can be greater than one, as is the case with voltage pumps, less than one, as in the case of regulated supplies, and negative, as in the case of negative charge pumps. All of these potentials require control and regulation to ensure proper operation of the die. The control of the supply ensures that the required potentials are available when the die needs it. The regulation portion of the equation ensures that the desired potential is sufficient to meet the circuit needs and can react to changes in the circuit using the potential.

This research explores the use of a Delta-Sigma Modulation-based circuit to control and regulate the operation of a voltage-generation circuit as well as introduce the ability to dynamically program the output voltage. What is presented in this thesis is the use of Delta-Sigma Modulation to sense, generate, and control the pumped wordline potentials necessary in a modern NAND memory device. These voltages generally consist of a read, erase, pass, and program potentials. The topology was chosen for voltage stability, superior response time when measured at the highest potential, and the ability to program the desired output potential depending on the circuit operation being performed.

The proposed circuit was designed and fabricated using AMI's 500 nm process through the MOSIS service (www.mosis.com). The chip performance has been evaluated and compared to the simulation results to verify accurate voltage generation over a wide input voltage and output response to changes in the input voltage. The control voltage was varied from 0.6 volts to 2.0 volts and the output voltages were measured to be 5.76 volts and 20.03 volts, respectively. The linearity of the output response was measured to average within 100 millivolts of the ideal. The response time of the DSM was also measured with good correlation to the simulation values.

TABLE OF CONTENTS

ACKNOWLEDGEMENTS	vi
ABSTRACT	viii
LIST OF TABLES	xii
LIST OF FIGURES	xiii
CHAPTER ONE: INTRODUCTION	1
1.1 Motivation	1
1.2 Flash Cell Construction	3
1.3 Principles of Flash Memory Operation	5
1.3.1 Programming a Flash Cell	6
1.3.2 Erasing a flash Cell	8
1.3.3 Reading a Non-Programmed or Erased Cell	9
1.3.4 Reading a programmed Cell	10
1.4 NAND String Operations	11
1.4.1 NAND String Programming	13
1.4.2 NAND String Erase	14
1.4.3 Reading a cell in a NAND String	15
1.5 NAND Array	17
1.6 Challenges with NAND Array Operations	18
1.7 Thesis Contribution	22
CHAPTER TWO: VOLTAGE PUMP CONTROL METHODS	23
2.1 Current Pump Control Technology	23
CHAPTER THREE: DELTA SIGMA MODULATION	28
3.1 DSM Theory of Operation	28

3.2 DSM for Voltage Pump Control	31
3.2.1 Generalized Explanation of the Circuit	32
3.2.2 DSM Pump Control	35
3.2.3 Developing the Delta Signal	35
3.2.4 Developing the Sigma Signal	36
3.2.5 Connecting Delta to Sigma	37
3.2.6 Delta-sigma operation	38
3.2.7 Complete Circuit	39
CHAPTER FOUR: CHIP TEST RESULTS	41
4.1 simulation and Experimental Methodology	41
4.1.1 Charge Pump Testing	45
4.1.2 Transient Response Analysis	46
4.1.3 Delta V_{in} Sensitivity	50
4.1.4 Linearity	52
4.1.5 V_{out} Ripple	52
4.1.6 Summary	54
CHAPTER FIVE: CONCLUSIONS AND FUTURE WORK	55
5.1 Conclusions	55
5.2 Future Work	56
REFERENCES	58

LIST OF TABLES

Table 1.	Data for DSM Sample Data	31
Table 2.	Package Pin Assignments	44

LIST OF FIGURES

Figure 1.	Flash Cell Construction	3
Figure 2.	TEM Image of a Modern Flash Cell	4
Figure 3.	Storing Charge on the Floating Gate	6
Figure 4.	Programming a Flash cell with Fowler-Nordheim Tunneling	7
Figure 5.	Erasing a Flash Cell with Fowler-Nordheim Tunneling	8
Figure 6.	Reading a Non-Programmed or Erased Cell	9
Figure 7.	Reading a Programmed Cell	10
Figure 8.	NAND String with 32 Cells in Series	11
Figure 9.	Simplified NAND String with 5 Flash cells	12
Figure 10.	Schematic of simplified NAND string	13
Figure 11.	Programming a cell in a NAND string	14
Figure 12.	Erasing cells in a NAND string	15
Figure 13.	Reading a non-Programmed cell	16
Figure 14.	Reading a Programmed cell	17
Figure 15.	NAND Array Architecture	18
Figure 16.	Programming a cell in the mini-array	19
Figure 17.	Cells unintentionally programmed along the wordline	20
Figure 18.	Voltage Pump with Control Circuitry	23
Figure 19.	Sample Voltage Pump Control Circuit	24
Figure 20.	Simple Regulation Circuit	25
Figure 21.	Pump controller with programmable Input Voltage	26
Figure 22.	Simple Analogy of DSM	28
Figure 23.	Simplified Schematic of DSM Pump Control Circuit	32

Figure 24.	Schematic of DSM Pump Control Circuit with Pump Delay	34
Figure 25.	DSM Controlled Charge Pump	35
Figure 26.	Switched Capacitor Circuit (Delta)	36
Figure 27.	Integrating Amplifier, Sigma stage	37
Figure 28.	Complete Delta-Sigma Circuit	37
Figure 29.	Current path when V_{in} is greater than V_{fb}	38
Figure 30.	Current path when V_{in} is less than V_{fb}	39
Figure 31.	Completed Schematic of DSM controlled High Voltage Pump	40
Figure 32.	Feedback network schematic	40
Figure 33.	Die floor plan and pin assignment	42
Figure 34.	Chip photograph	43
Figure 35.	Characterization bench setup	45
Figure 36.	Charge pump layout	46
Figure 37.	Charge pump photograph	46
Figure 38.	DSM response to V_{in} level change 0 V to 0.75 V	47
Figure 39.	Response time to start up	48
Figure 40.	DSM controller response to varying output conditions	49
Figure 41.	DSM detecting a V_{in} change of 100 mV	51
Figure 42.	V_{out} Linearity with V_{in}	52
Figure 43.	V_{out} Ripple with varying load capacitance	53

CHAPTER ONE: INTRODUCTION

1.1 Motivation

The advancement of semiconductor devices and their applications have driven the need to shrink the devices as well as enable their application in more diverse and demanding environments. One significant area of employment has been in the mobile environment. In this arena the power consumption of every component in the application is scrutinized for the utmost efficiency. The average power as well as the peak power is analyzed in detail to ensure that every component is operating at peak efficiency.

In order to optimize the efficiency of every component in the system the requirements for an efficient and highly optimized circuit design are placed on each design. This requires a significant effort on the part of the circuit designer to evaluate every sub-circuit of each chip to ensure that it is as efficient as possible. One area of examination is the generation of the necessary on-chip potentials that are used in the course of operating the device.

In modern NAND devices, there are a number of potentials generated internally. These include an elevated potential that is used for programming or erasing the NAND cells. This is the program potential and can range as high as +20 volts in order to properly program the NAND cell. Another potential is the read potential. This potential is used to determine the threshold voltage of the cell. This is then interpreted by the

sensing circuitry to determine the contents of the cell. Another potential is the pass potential, which is used to set the voltage on all the remaining cells along the NAND string to the potential required to pass current so that the selected cell can be read. Other voltages necessary in modern NAND devices are the program and program inhibit voltages [4]. This diversity of required potentials that are necessary has been addressed by the design and implementation of various voltage generation supplies within the chip. Each chip can require up to 7 different supply voltages in order to operate properly [2]. Other designs use fewer circuits and inefficient methods of generating the intermediate potentials necessary for proper operation. The regulation and control of the various potentials must also meet stringent requirements for set point and ripple.

The voltage generation circuit in this work addresses the need for numerous potentials on the die as well as simplifying the design of the circuit itself. In this work a Delta-Sigma Modulator (DSM) controller connected to a charge pump is used to generate the positively pumped potentials that are necessary for the normal operation of the NAND device.

The use of a DSM front end to control and regulate the operation of the charge pump introduces the opportunity to reduce the number of pump circuits on the die to exactly the number necessary for normal operation. Additional benefits are better control of the potential, decrease in overall chip area and a decrease in the power consumption of the die.

1.2 Flash Cell Construction

The essential elements in the construction of flash cells are the control gate, a floating gate, barrier oxide, tunnel oxide and a standard silicon substrate with source and drain implant areas. In Figure 1 a basic flash cell is illustrated showing these elements of a flash memory cell. These elements are stacked vertically and form the flash cell

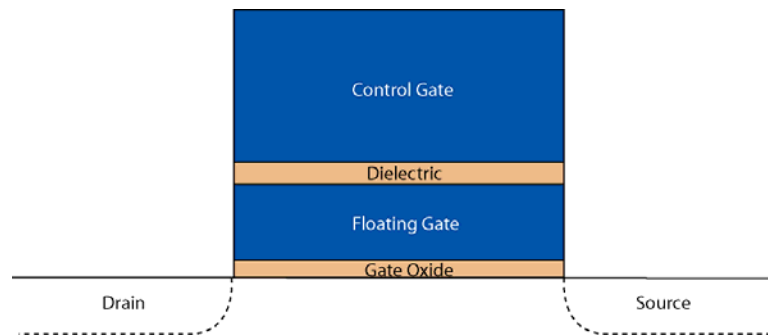


Figure 1. Flash Cell Construction

The control gate is the (polysilicon) conductor that is used to access and program the flash cell. The necessary bias voltages are applied to this node to control the flash memory cells behavior. The dielectric between the control gate and the floating gate serves as a conduction barrier between these two nodes. As will be demonstrated in the operations section this primarily serves as a capacitor dielectric between these nodes. The floating gate is the conducting, or in some cases semi-conducting, layer that is used to store charge and alter the threshold voltage of the flash cell. The lower oxide, commonly called the gate oxide or tunnel oxide is used to separate the floating gate from the substrate. It is this oxide that electrons tunnel from the channel to the floating gate, as

in a program operation, and from the floating gate to the substrate, as in an erase operation.

The source and drain regions on either side of the flash cell are other locations where desired potentials are applied and connect the flash cell to other flash cells in the creation of a memory array.

The TEM image in Figure 2 shows is a modern flash cell. In this image the control gate is fabricated from silicided polysilicon and is located above the barrier oxide. The dark region on top of the control gate is Tungsten silicided polysilicon. The width of the device is 42 nm. The floating gate can be seen sandwiched between the barrier oxide and the tunnel oxide. The barrier oxide must be thin enough to allow for good capacitive coupling to the floating gate but thick enough to prevent tunneling between these two nodes.

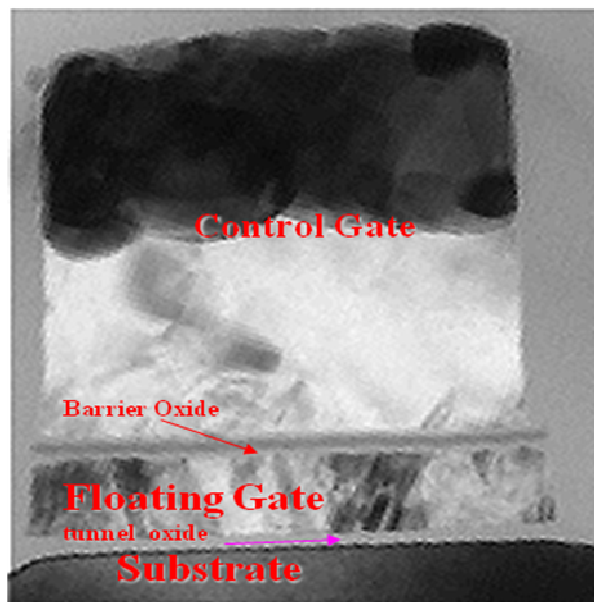


Figure 2. TEM Image of a Modern Flash Cell

The tunnel oxide can be seen below the floating gate and above the substrate. This oxide must be thin enough to present a low barrier to tunneling and yet be thick enough to have sufficient durability in operations.

1.3 Principles of Flash Memory Operation

A flash memory device stores information in an array of floating gate memory cells. These cells store charge through the process of adding or removing charges to and from the floating gate of the flash cell. This movement of charges alters the threshold characteristic of the device and thus allows for the programming of a cell so that current will either flow through the cell or be blocked during the read procedure. For the purposes of this thesis the flow of electrons from the source to the drain of the device is interpreted as a “1” and the absence of current flow is interpreted as a “0” on the floating gate.

Figure 3 illustrates the effect of storing charge on the floating gate on the threshold of the device. As the number of electrons that are added to the floating gate increases, the threshold voltage of the device is altered. If a sufficient number of electrons are added to the floating gate the device threshold grows and ultimately the device will be incapable of creating a channel and no current will flow in the device. This would result in a “0” being read out of the cell. The inverse case would be that there were no electrons stored on the floating gate, the cell is erased, and a channel can easily be formed in the device.

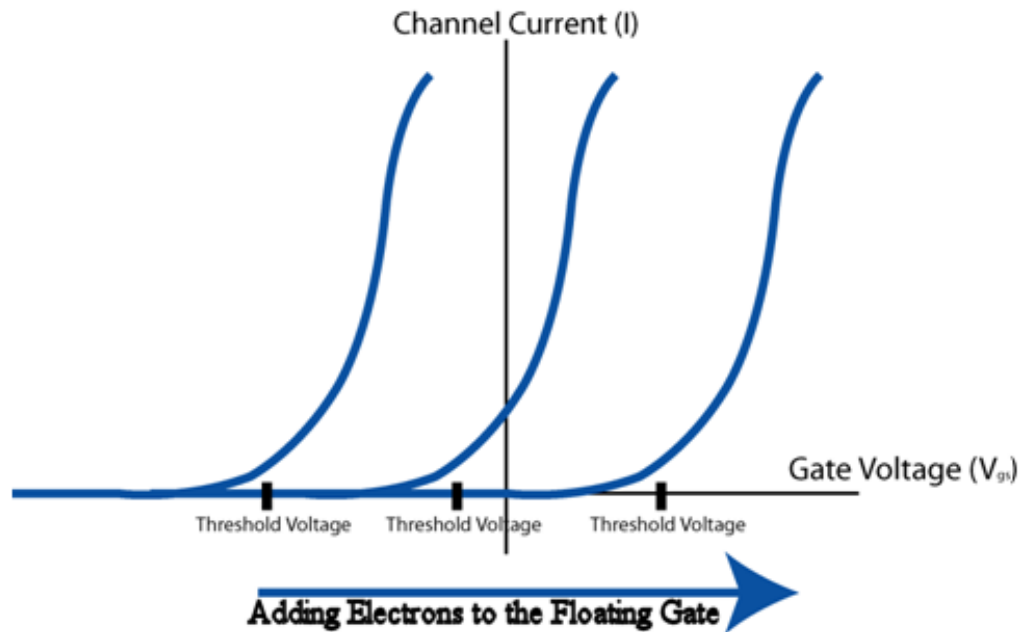


Figure 3. Storing Charge on the Floating Gate

1.3.1 Programming a Flash Cell

In order to properly describe flash memory operations it is necessary to understand the primary mechanisms whereby flash cells operate. The first operation to understand is how a flash cell is programmed. As was described in the previous section, flash memory is programmed by altering the threshold voltage of the cells so that the threshold voltage is above or below the read potential programs flash cells. The primary mechanism through which this is achieved is Fowler-Nordheim- Tunneling, FNT [7]. Figure 4 shows the method of how the flash cell is programmed using this mechanism.

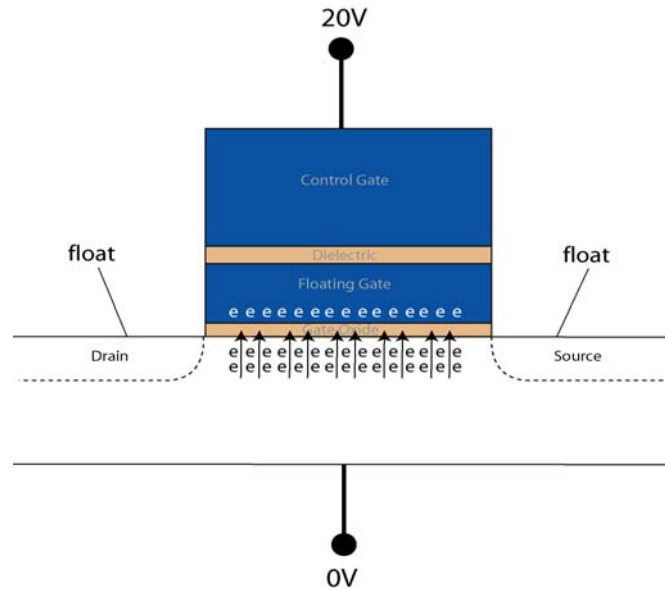


Figure 4. Programming a Flash cell with Fowler-Nordheim Tunneling

A high potential, for example, +20 V, is applied to the control gate of the cell and this potential capacitively couples to the floating gate, increasing its potential. The drain and the source contacts are floating. The substrate is tied to a reference potential, typically ground, and electrons are drawn up from the substrate, through the tunnel oxide and into the floating gate. The increase in electrons on the floating gate raises the effective threshold voltage of the device. The standard CMOS threshold voltage equation can be modified to include the effects of the trapped charges present in the floating gate.

This term is the $\frac{Q'_{poly}}{C_{ox}}$ term in the threshold voltage equation 1.1[7].

$$V_t = \left(-\phi_{ms} - 2\phi_{fp} + 2 \left(\frac{Q'_{b0}}{C'_{ox}} + \frac{Q'_{poly}}{C'_{ox}} \right) \right) \quad 1.1$$

1.3.2 Erasing a Flash Cell

The erase procedure is effectively the same procedure as the program operation except that the potentials are reversed. Figure 5 illustrates the flow of electrons from the floating gate to the substrate during this operation.

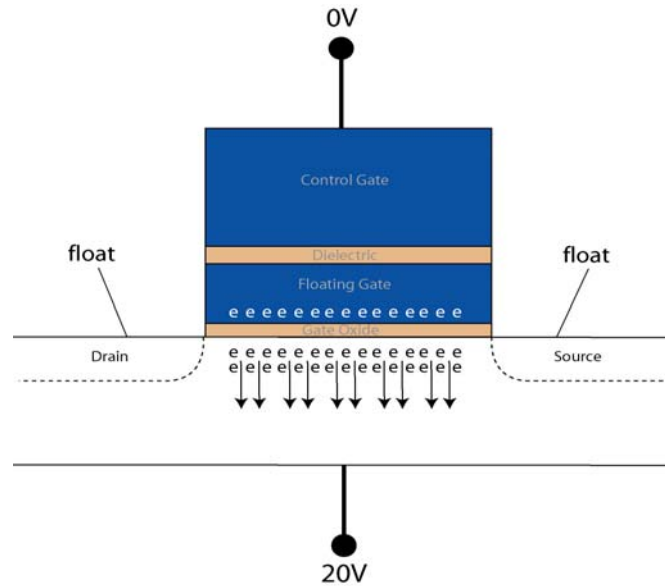


Figure 5. Erasing a Flash cell with Fowler-Nordheim Tunneling

The control gate is placed at ground, the source and drain contacts are floating and the substrate is set to +20 V. This causes the electrons that were trapped on the floating gate to tunnel back through the tunnel oxide and into the substrate. This lowers the threshold voltage of the flash cell.

1.3.3 Reading a Non-Programmed or Erased Cell

A non-programmed cell has the floating gate in a condition where it has no electrons stored upon it. This is also the desired state of the floating gate after an erase condition. Refer to Figure 6 for the device conditions.

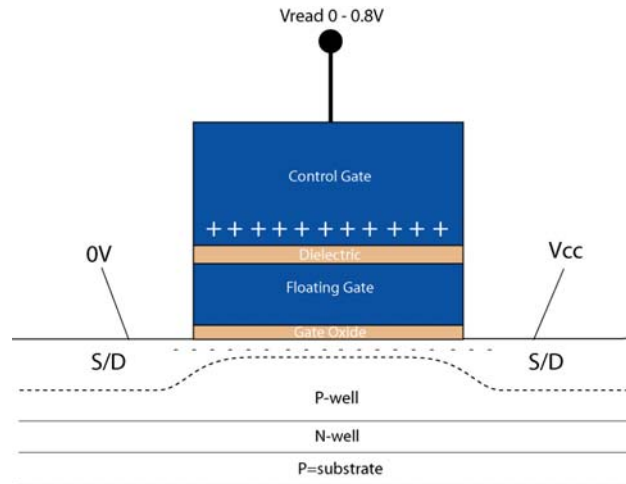


Figure 6. Reading a Non-Programmed or Erased Cell

For the purposes of this discussion we will assign a threshold voltage of the device of -1 V when in the non-programmed condition. To read this cell a bias is applied to the drain of the device and a reference potential, ground, is applied to the source of the device. The read potential is then applied to the gate. This potential is set at a level sufficient to form a channel below the gate when the cell is not programmed and insufficient for channel formation when the cell is programmed. For this example it is set at 0.8 Volts. The channel is formed between the source and drain thereby creating a conductive channel between these nodes. A sensing circuit is then used to determine that

the current was able to flow from the source to the drain of the device indicating a “1” stored in the cell.

1.3.4 Reading a Programmed Cell

A programmed cell is one in which charges have been stored on the floating gate, thereby raising the threshold voltage of the device. Refer to Figure 7 for the device conditions.

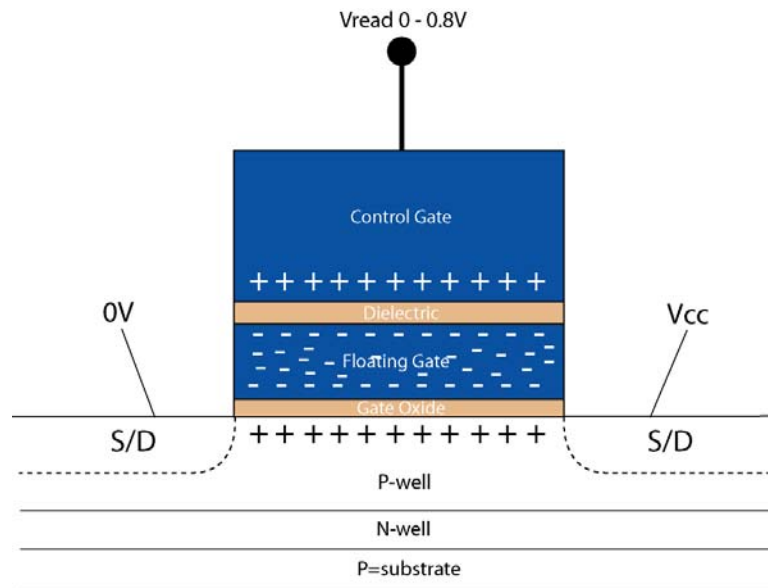


Figure 7. Reading a Programmed Cell

In this condition the threshold voltage of the device has been altered to be greater than 0 V. For this illustration it will be 3.0 V. This read operation is procedurally similar to the one previously described. A bias is applied to the drain of the device and a reference potential, ground, is applied to the source of the device. The read potential is then applied to the gate. This potential is once again set at 0.8 Volts, a level sufficient to

form a channel below the gate when the cell is not programmed and insufficient for channel formation when the cell is programmed. Since this is insufficient to form a conductive channel between the source and drain, $V_{gs} < V_{th}$, current cannot flow from source to drain. The sensing circuit now determines that the current was not able to flow from the source to the drain of the device indicating a “0” is stored in the cell.

1.4 NAND String Operations

Modern NAND memory devices are created from sets of NAND strings. Figure 8 is SEM image of a modern NAND string that is 32 cells long. Current technology has NAND strings that are 32 Flash cells long and strings as long as 64 cells have been proposed [1], [10].

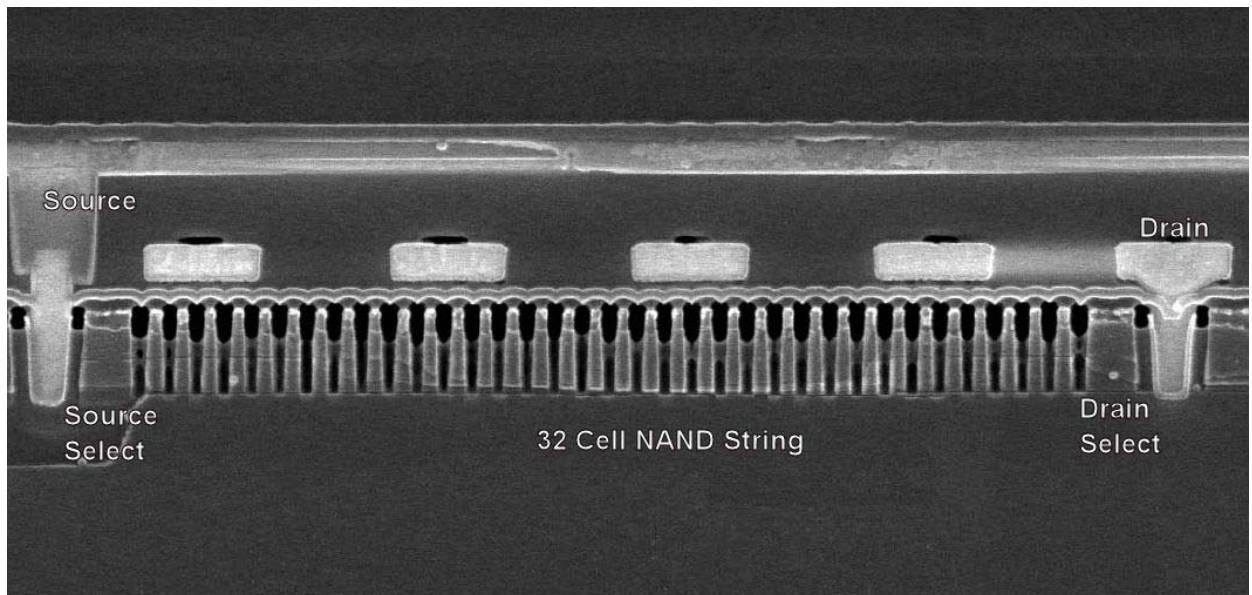


Figure 8. NAND String with 32 Cells in Series

Another technological advance has been the ability to store more than 2 levels in a given cell. This technology, Multiple Level Cell, MLC, allows for the manufacturing of

devices with greater than 100% array efficiencies [1]. NAND devices have been proposed that use 16 different threshold levels per cell to create a 16 Gb device [12]. A complete NAND string consists of the series connection of the flash cells, a source select device, a drain select device, and a precharge device. The entire string can be manufactured in a compact form allowing for a significant increase in the bits/cm².

For the purposes of the following discussion simplified version of the NAND string will be used. This string will have 5 flash cells along with the necessary select devices used to access the NAND string. This representation is shown in Figure 9.

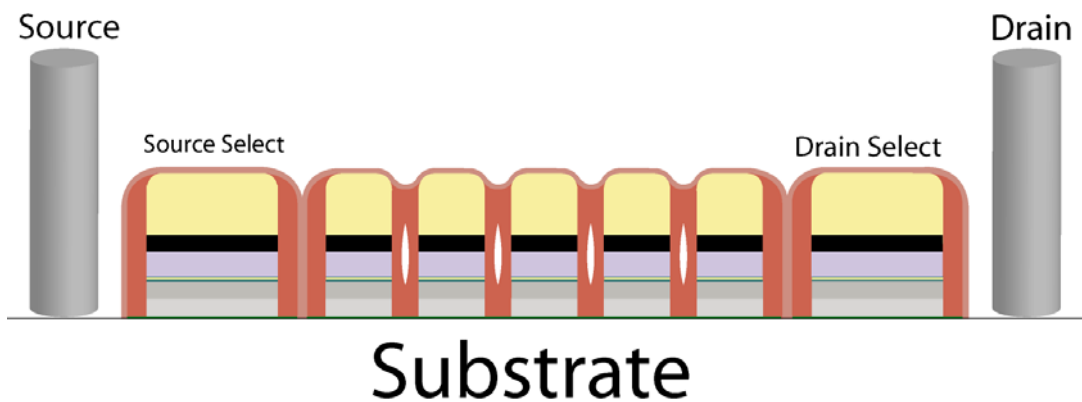


Figure 9. Simplified NAND string with 5 Flash cells

Figure 10 shows the corresponding schematic of this simplified NAND string. The threshold voltage of an erase cell will be -3 V and a programmed threshold voltage will be $+4$ V.

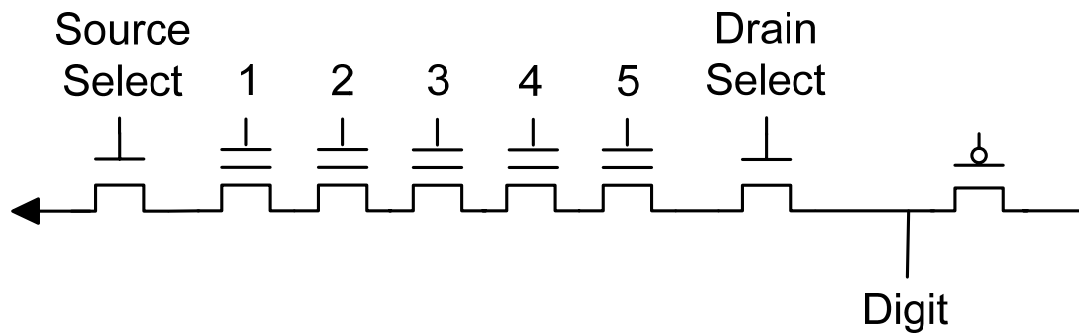


Figure 10. Schematic of simplified NAND string

1.4.1 NAND String Programming

The programming operation in a NAND string will increase the threshold voltage of one cell and not change the potential on the floating gates other cells in the string. In order to accomplish this, another potential must be introduced. This is an inhibit potential that prevents the cells adjacent to the desired cell from being programmed while the desired cell is programmed [4]. The inhibit potential is high enough to prevent the unselected cells from being programmed and low enough to prevent threshold voltage alteration of these cells. Figure 11 illustrates this condition.

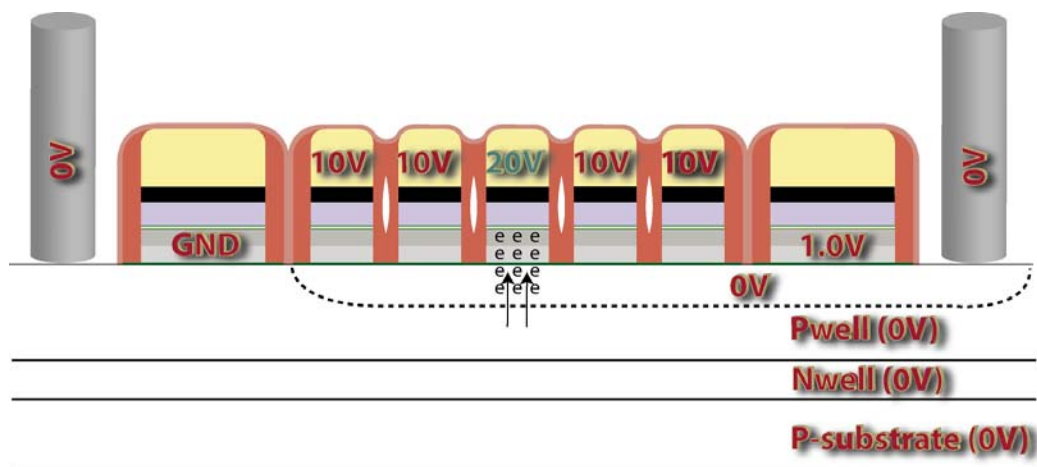


Figure 11. Programming a cell in a NAND string

In this Figure 11, cell number 3 will be programmed and the remaining cells will not be programmed. The gate voltage of cell number three is set to +20 V, the programming voltage. The remaining cells along the string are set to +10 V, the inhibit voltage. The substrate must be set to 0 V. To accomplish this, the drain select device is turned on and the bitline potential is set to 0 V. This sets $\sim+20$ V across the device to be programmed and $\sim+10$ V across the non-programmed cells. Electrons tunnel through the tunnel oxide and into the floating gate, raising the threshold voltage of the programmed cell.

1.4.2 NAND String Erase

The erase operation is similar to the program operation. In NAND arrays the cells are all erased in a block. This means that a give section of the array, not individual cells, must be erased at once. The potentials that are necessary must be sufficient to drive the electrons trapped in the floating gate out and back into the substrate. The substrate is

driven to +20 V and the wordlines in the string are all set to 0 V. This will erase the entire block of memory at once. Typical NAND block sizes are 135.2 kB [11].

Figure 12 shows the block erase technique. There are 4 cells that are programmed and one cell that is not programmed.

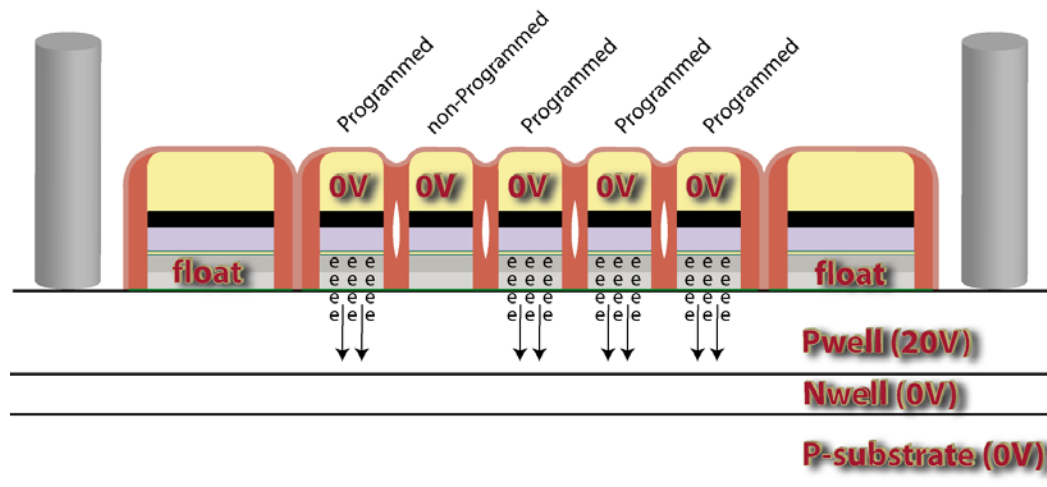


Figure 12. Erasing cells in a NAND string

The substrate, in this case a p-well, is driven to +20 V and all the wordlines are set to 0 V. This causes the electrons stored on the floating gates to be attracted to the substrate. They pass through the tunnel oxide and into the charge pump generating the +20 V potential.

1.4.3 Reading a cell in a NAND string

The cells in this sample NAND string can have two states, programmed and erased. It is important to understand the mechanisms whereby each state is read. Here

the procedure for reading both states is described. In both cases the digit line is precharged to a known level. This level is determined during the design phase and is merely a reference whereby the cell value can be determined in the sensing operation.

In reading a cell that is not programmed, the threshold voltage is at ~ -4 V. The read potential, 0 V, is applied to the gate of the desired cell. The pass potential, 4.5 V, is applied to all the other cells in that string. The pass potential is high enough so that even if a cell is programmed, threshold voltage at ~ 3 V, the cell will still be turned on and form a channel beneath the gate and yet low enough to prevent programming the cell. Figure 13 illustrates how this is accomplished. Cell three is not programmed and receives the same read potential, 0 V in this example. Since the threshold voltage for this cell is at ~ -3 V this is sufficient for the formation of the channel.

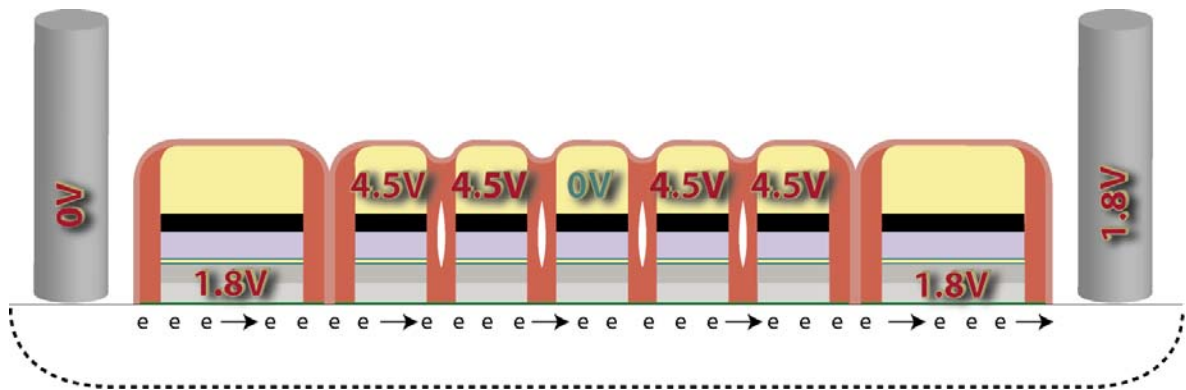


Figure 13. Reading a non-Programmed cell

The pass potential applied to the gates of the remaining cells. Since their threshold voltage is less than 3 V a conductive channel is formed below the remaining cells in the string. The source select and the drain select devices are enabled to connect

the string to the reference potential and the bitline, respectively. The NAND string now has a complete conduction path from the bitline to ground. This causes the bitline voltage to decrease and is sensed at the end of the array.

The process of reading a programmed cell is the same as reading a non-programmed cell. The bitline is precharged to a known level and the pass potential is applied to the non-selected cells. The source select and drain select potentials are the same and connect the string to ground and the bitline. The read potential, 0 V, is once again applied to the cell of interest. Figure 14 illustrates the NAND string condition for this case. The middle cell is the one that is programmed and has a threshold voltage of ~ 3 V. Since the read potential is 0 V this is insufficient for channel formation below the gate.

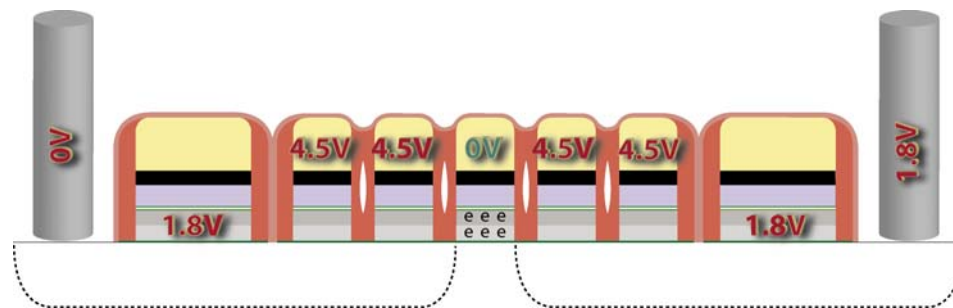


Figure 14. Reading a Programmed cell

1.5 NAND Array

It can be seen that connection a number of NAND strings together would enable the creation of highly dense array architecture. This array of the example NAND Strings is illustrated in Figure 15. In this figure there are four sets of our primitive arrays

connected together. In order to improve array efficiency the arrays share common source and drain connections. For example the source connection in the center of the array is shared between the two adjacent array sections. The source select and drain select devices are highlighted in purple.

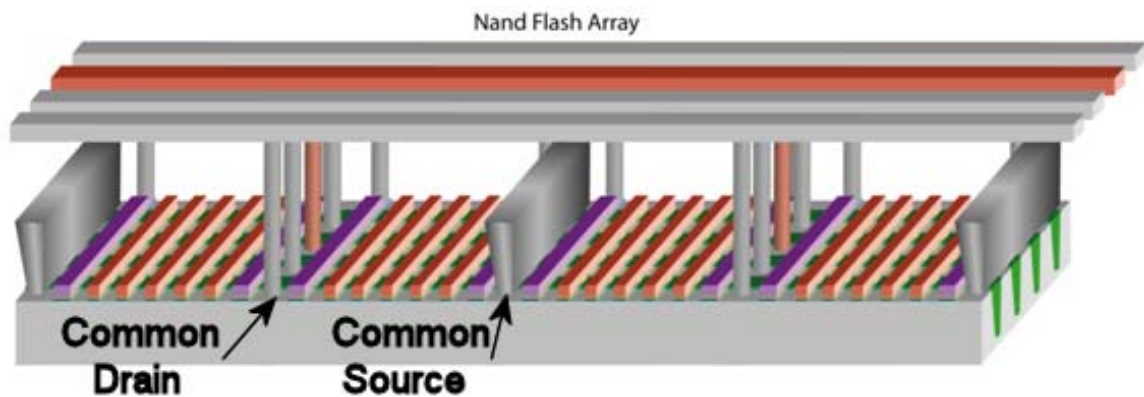


Figure 15. NAND Array Architecture

1.6 Challenges with NAND Array Operations

As the industry drives to increase the number of cells per unit area, cells/cm², the proximity to the adjacent cells decreases. This causes issues related to unintentional programming or program disturb of the cells not selected for the programming operation. These issues are unintentional programming along the desired wordline [9], unintentional programming of adjacent cells [3], Gate Induced Drain Leakage, GIDL, and Band to Band tunneling that can occur. These program disturb effects are countered with different program inhibit schemes. In order to illustrate the program disturb effects in Figure 16 we have selected a cell for programming in the mini-array. This wordline will be driven

to the program potential and the non-selected wordlines are set to the program inhibit potential.

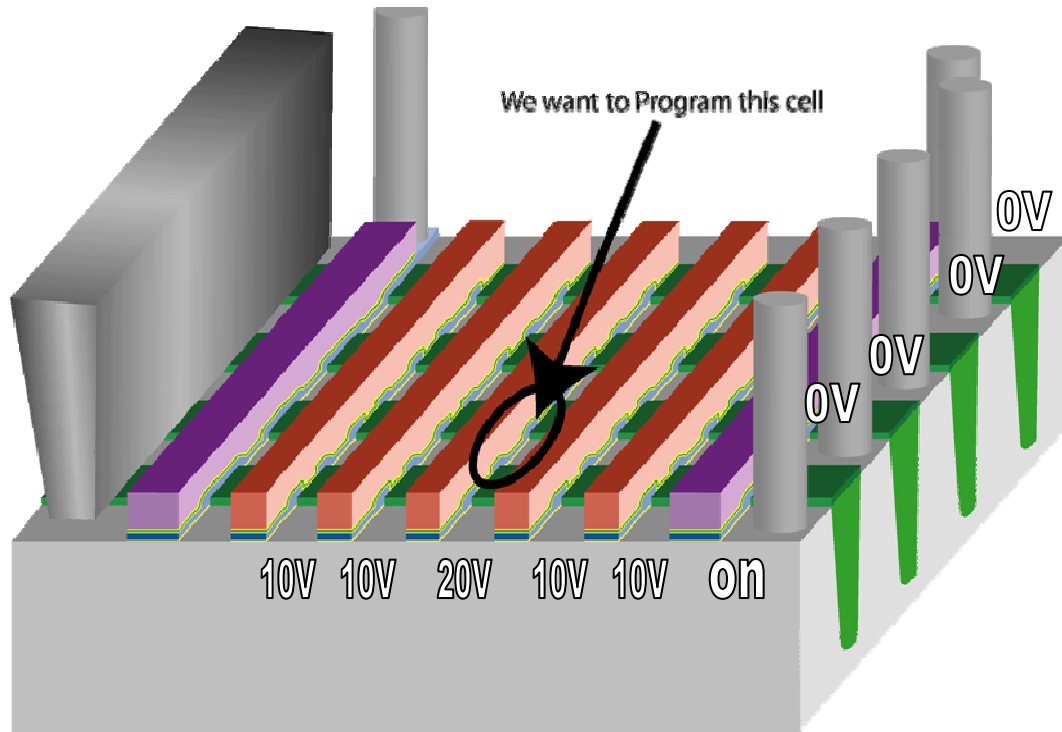


Figure 16. Programming a cell in mini-array

Recall that in the programming operation the selected wordline is driven to +20 V and the adjacent word lines are driven to +10 V. Electrons are attracted into the floating gate of the selected cell and then the program operation is terminated. However, due to the fact that the entire wordline received the +20 volt potential, the remaining cells along that wordline were also programmed. Figure 17 shows the cells that were unintentionally programmed along the wordline.

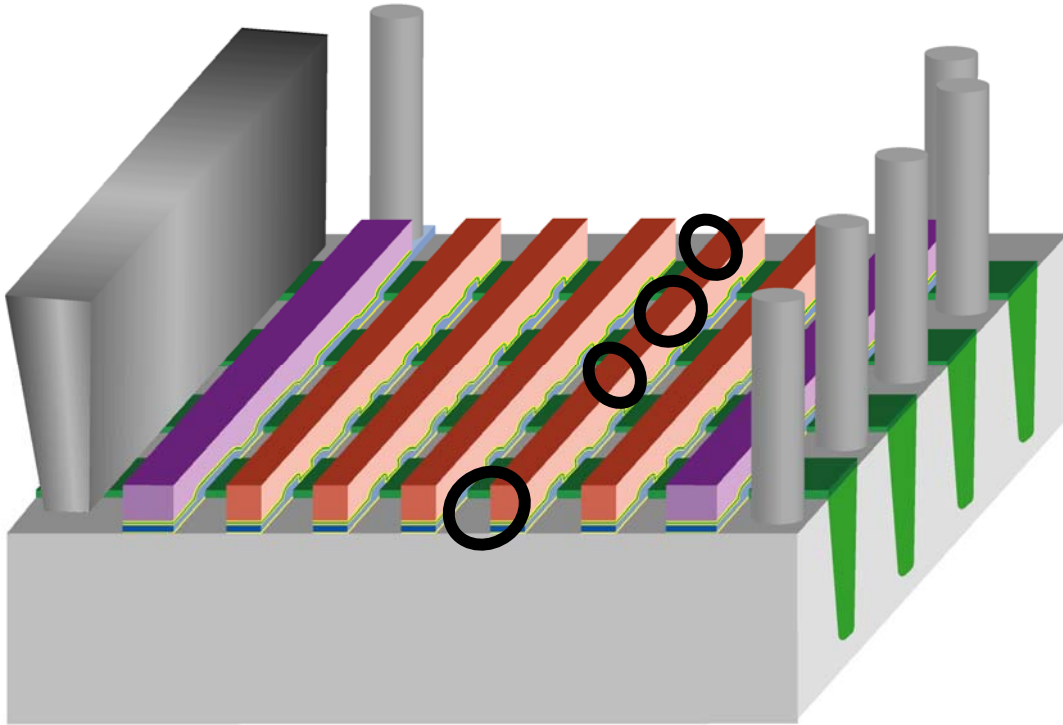


Figure 17. Cells unintentionally programmed along the wordline

Numerous solutions have been proposed to mitigate these effects. Boosting schemes have been proposed [5] whereby the voltages of adjacent wordlines and bitlines are modulated. There are also circuit methods introduced to modify the source potential in order to mitigate the program disturb effects [2], [3]. Various architectures have also been implemented in order to reduce the unintentional alteration of the threshold potential of the adjacent cells. Toshiba has implemented an All Bit Line, ABL, architecture in which each bit line has its own sensing amplifier circuitry. This increases the SNR on the selected bit lines. Micron has introduced an architecture in which the page buffers are centered on the array [1]. This reduces the bit line length and the loading on the sensing circuitry.

Another method of increasing the cells/cm² is to increase the number of bits that can be stored in each cell. In this multi-level cell design requires that the threshold values of the flash cells to be adjusted and sensed on the order of hundreds of millivolts. The storage of two bits per cell is current technology and the storage of 3 and 4 bits per cell is leading edge [1]. Storing two bits per cell requires the establishment of four different threshold values in each cell. This is accomplished through accurate program potentials and complex algorithms to determine the state of the cell. One proposed architecture is one in which a 1.8 V process is used and there are 16 different levels available in each cell [12]. This requires that the programming voltages be adjusted in the 100 mV realm.

Each of these methods implemented to reduce the unintentional programming of non-selected cells requires the generation of accurate potentials that can be used to program or inhibit the programming of the cells in the array. Voltage charge pumps are designed and implemented that generate these potentials. In many cases dedicated pump circuitry is designed for each desired potential. If intermediate potentials are necessary then they are derived from the dedicated pumps. One example would be the generation of the pass potential, +10 V. This has been generated from the +20 V program potential through the use of a voltage divider and regulation circuits. This wastes power in the generation of twice the desired potential as well as power in the wasting of half that power in the divider circuit.

A dynamically programmable voltage pump would reduce the necessity to over generate the desired potential and decrease the power wasted in the die. It could also

decrease the overall area requirement for the voltage pumps on the die though more efficient use of current pumps.

1.7 Thesis Contribution

This Thesis looks at the use of Delta-Sigma Modulation, DSM, based control of a voltage pump. The operation of the DSM control of the voltage is explained and demonstrated. Comparison to standard fixed potential generators is also examined. Special attention to the ability to program the voltage pump to desired levels and response time of the pump to control inputs are analyzed and demonstrated.

CHAPTER TWO: VOLTAGE PUMP CONTROL METHODS

2.1 Current Pump Control Technology

Modern charge pumps are controlled with relatively basic on/off regulation. The desired potential is generated and a portion of this is fed back into a regulation circuit. The output of the regulation circuit either enables or disables the pump in some manner. Figure 18 is a block diagram of a voltage pump with the pump controller and the feedback path.

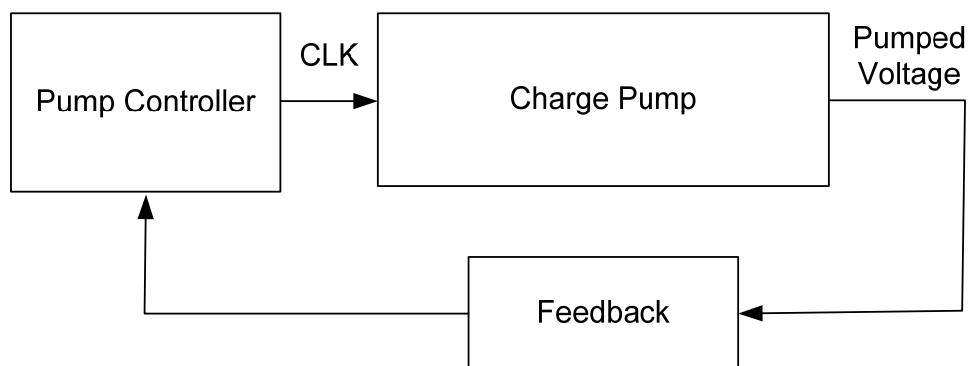


Figure 18. Voltage Pump with Control Circuitry

The pump controller is designed with a desired set point that is specified and then trim circuits are added to allow for manufacturing variations in circuit performance. The output of this circuit is a steady pumped voltage at a fixed level. An example pump control circuit is detailed in Figure 19 [7]. The high voltage bias string is used to

that operates the charge pump. The control circuit could have adjustable components in the circuit but once trimmed it would remain at a fixed value.

If other pumped values are desired then the pumped value can be regulated down to the desired level. Figure 20 shows a simple regulation circuit. The disadvantage to this circuit is that the pumped voltage must be generated and then regulated down to the desired potential. This wastes valuable energy due the requirement of generating a pumped voltage that is higher than necessary.

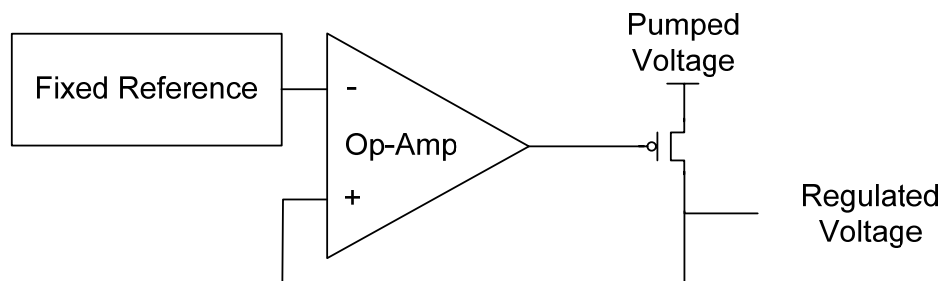


Figure 20. Simple Regulation Circuit

Another method of modulating the pumped value is to introduce a voltage that controls the value of the charge pump [9]. This control value can be adjusted based on the needs of the circuitry using the charge pump voltages. Figure 21 illustrates the concept of having a controllable voltage determine the pumped voltage value.

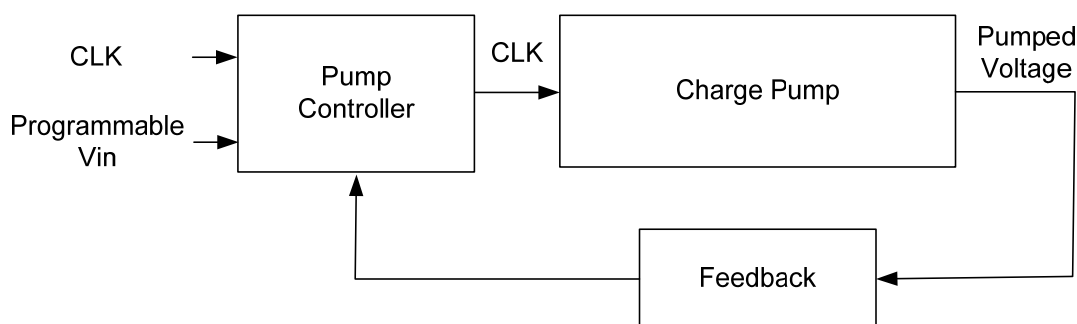


Figure 21. Pump Controller with programmable Input Voltage

This is common practice in NAND devices where precise adjustment of the threshold value is desired. In Multi-Level-Cell, MLC, devices the threshold value of the cell must be set to one of many different values. During the program phase of operations the internal algorithm of the device performs a program operation and then reads the cell to determine whether or not the cell is at the desired level. If the cell has not yet reached the desired level then another programming operation is executed until the read operation results match the desired programming value. In advanced NAND devices the programming voltage is actively adjusted to properly program the cell to the desired threshold voltage [9]. This has an added benefit of preventing a condition called over-programming. Over-programming occurs when the threshold value is set at a level

beyond the desired level and results in a data error. In order to correct this condition the entire block must be erased and reprogrammed or error correction methods must be used to compensate for the over programmed cells.

CHAPTER THREE: DELTA SIGMA MODULATION

3.1 DSM Theory of Operation

Delta Sigma Modulation works by translating a value to be measured into a flow rate and converting that flow rate into an average value. The key steps to the process are the conversion of the value to be sensed into a proportional flow rate and then determining the value of that flow rate over time. This value can then be used to determine the average flow rate and that value can be related back to the value that is being measured. Figure 22 shows a simplified analogy of how Delta Sigma Modulation works.

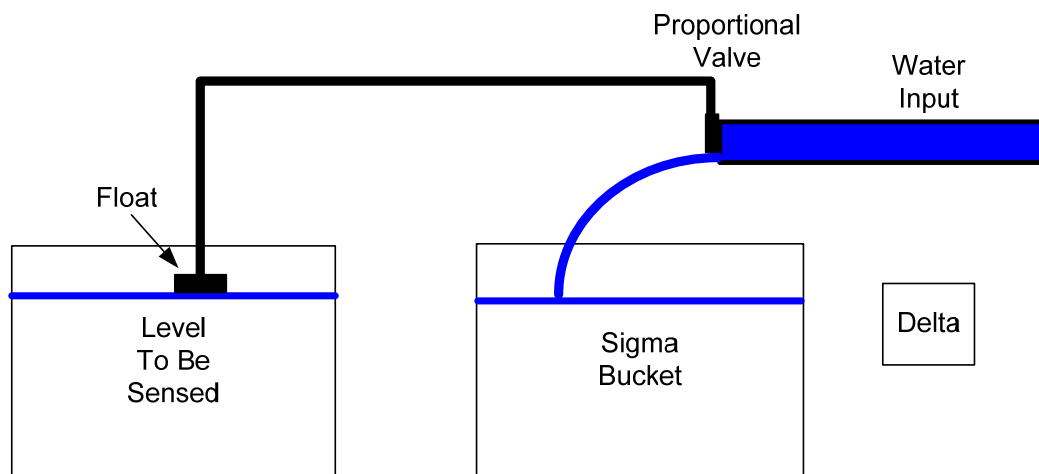


Figure 22. Simple Analogy of DSM

This analogy uses four simple components to demonstrate how the Delta Sigma Modulation works. There is the container with the unknown value of water to be

measured, the Sigma bucket, the proportional valve that controls the flow rate into the Sigma bucket and the Delta cup. As the water level in the sensing bucket changes this opens and closes the proportional valve adjusting the flow rate of the water into the Sigma bucket. The Delta cup is a precisely determined amount that will be conditionally removed from the Sigma bucket at periodic intervals. This is important as the accuracy of the Delta value and the timing of the sampling is critical to the overall accuracy of the system.

As the unknown water level changes the valve opens and closes adjusting the flow rate into the Sigma bucket. In the Sigma bucket there is a sensor that determines whether or not to remove a Delta cup amount of water from the Sigma bucket. The position of this sensor is not important, just that it accurately and reliably determines the level in the Sigma bucket and communicates this to the Delta cup. As the water level rises the level is sensed and a decision is made whether or not to remove a Delta cup of water from the Sigma bucket. As the number of samples increases we can develop a signal based in the sample rate and the number of times we removed a Delta cup from the Sigma bucket. This signal becomes the average flow rate of water into the Sigma bucket and it represents the relative height of the water in the bucket.

In order to translate the conditional output bit stream into a meaningful data set we connect the sample decision bit stream to a counter. When the decision is made to remove water from the Sigma bucket, meaning that the water level in the Sigma bucket is less than the unknown value, the counter is incremented. If the decision is made not to remove water from the Sigma bucket, the counter is not incremented.

As this value builds over time the bit stream converges on the average amount of water that was removed from the bucket, which represents the average rate at which water flows from the proportional valve. This flow rate is representative to the weight of the unknown item.

An example would be if the rate that the water is flowing into the Sigma bucket is one cup every 30 seconds. If we sample the Sigma bucket every 10 seconds then the average flow rate should be 0.33 cups every 10 seconds. The Delta cup is set at 1 cup. If the sensing starts at an arbitrary level in the sigma bucket of 10 cups we can generate the desired bit stream which can be used to calculate the flow rate of water into the Sigma bucket. Table 1 shows this data set for 15 samples. At the first sample point, 10 seconds, 0.33 cups have been put into the Sigma bucket. This is above the sense line so a Delta cup is removed from the bucket. The level in the Sigma bucket is now 9.33 cups. At the next sample point, 20 seconds later, 0.33 cups has been put into the Sigma bucket. Since this is below the sense line, 9.66 cups are in the Sigma bucket, the Delta cup is not removed. At the 30 second point the Sigma bucket contains 9.66 cups and the value is still below 10 cups so no Delta value is removed. The 40 second point the Sigma bucket now contains 10.32 cups so another Delta cup amount is removed from the Sigma bucket. As the number of samples increases we approach the average value of the flow rate, 0.33 cups per 10 seconds.

Table 1. Data for DSM Sample Data

Time (seconds)	Level in Sigma Bucket	Decision Bit Stream	Running Average
0	10		0
10	10.33	Yes	1.00
20	9.66	No	0.50
30	9.99	No	0.33
40	10.32	Yes	0.50
50	9.65	No	0.40
60	9.98	No	0.33
70	10.31	Yes	0.43
80	9.64	No	0.38
90	9.97	No	0.33
100	10.3	Yes	0.40
110	9.63	No	0.36
120	9.96	No	0.33
130	10.29	Yes	0.38
140	9.62	No	0.36
150	9.95	No	0.33

3.2 DSM for Voltage Pump Control

The Delta Sigma Modulation circuit in this implementation measures a proportional value of V_{out} , and converting this to a rate of flow, I_{in} . This flow of I_{in} is stored during each sampling period. This stored flow rate is then quantized over time by sampling the stored value of the flow rate.

This quantized value is then averaged over time to obtain an average flow rate that represents V_{out} . In this implementation the input value, V_{in} , is a voltage level that is proportional to the desired output voltage at a 10:1 ratio. That is $V_{in} = 0.1 * V_{out}$. The output voltage is fed back through a divider network to produce V_{fb} .

The value of $V_{fb} = 0.1 * V_{out}$. The difference between V_{in} and V_{fb} is converted into a rate of flow, I_{in} , and is stored on a capacitor. This stored charge represents the Delta value.

3.2.1 Generalized Explanation of the Circuit

A simplified implementation of the entire circuit is shown in Figure 23. The summation of the currents at the input to the Op-Amp are the input current, I_{in} , the feedback current, I_{fb} and the integrated value of the integrating amplifier, I_{outi} .

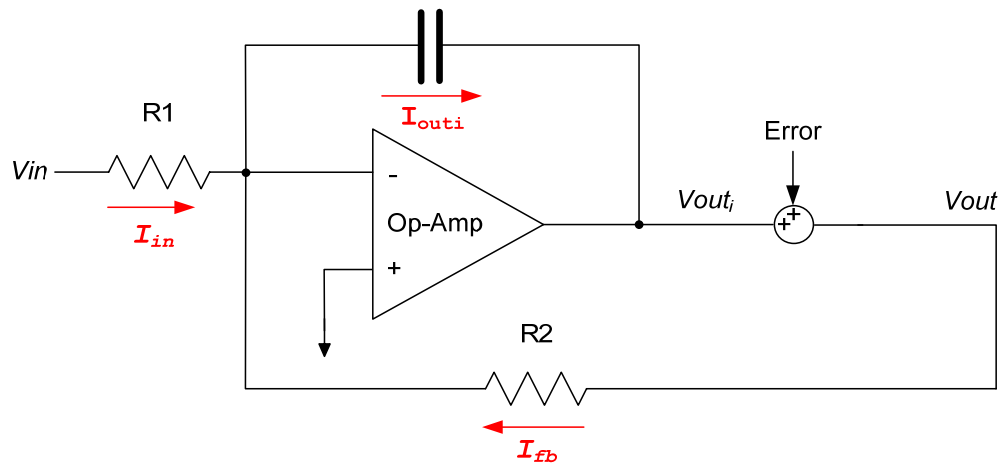


Figure 23. Simplified Schematic of DSM Pump Control Circuit

The summation of these currents at the input of the Op-Amp results in equation 3.1.

$$I_{in} + I_{fb} = I_{outi} \quad (3.1)$$

Converting this to the voltages and treating the op-amp as an ideal amplifier, $I_{in} = V_{in}/R$, results in equation 3.2.

$$\frac{V_{in}}{R_1} + \frac{V_{out}}{R_2} = \frac{-V_{outi}}{j\omega C} \quad (3.2)$$

The error that is introduced into the circuit through noise and device variations is lumped into the parameter Error, E_r , and is inserted at the output of the integrator. The sum of the error and the output of the integrating amplifier yield the output voltage, V_{out} .

$$E_r + V_{outi} = V_{out} \quad (3.3)$$

Substituting this result into equation 3.2 yields equation 3.4 with the variables V_{in} , V_{out} and E_r .

$$\frac{V_{in}}{R_1} + \frac{V_{out}}{R_2} = -(V_{out} - E_r) j\omega C \quad (3.4)$$

Solving equation 3.4 for the transfer function yields equation 3.5.

$$V_{out} = V_{in} \cdot \left(\frac{-\frac{R_2}{R_1}}{1 + j\omega R_2 C} \right) + E_r \cdot \left(\frac{j\omega R_2 C}{1 + j\omega R_2 C} \right) \quad (3.5)$$

This equation has two primary components. The first portion of the equation is the Signal Transfer Function, STF. The second portion of the equation is the noise Transfer Function, NTF. The STF portion is the Low Pass filter at DC is just the ratio of R_2 and R_1 . The NTF is a high pass filter, which at DC = 0.

The above derivations are with an idealized charge pump with no pump delay. In a real application there is a delay in the charge pumps ability to react to a circuit demand

for the pumped voltage and delay in the pumps ability to respond to changes in the programming voltage. Figure 24 shows the circuit with the incorporation of the pump delay.

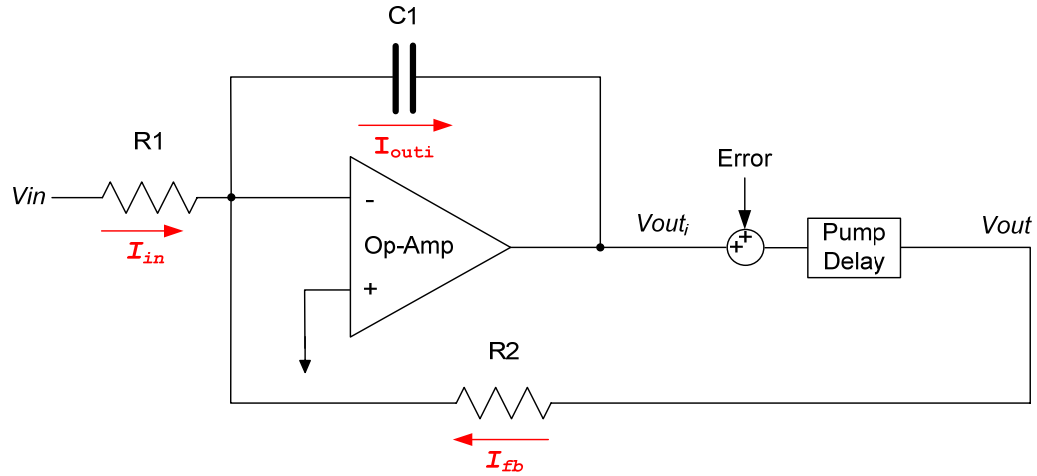


Figure 24. Schematic of DSM Pump Control Circuit with Pump Delay

This pump delay takes the form of equation 3.6.

$$V_{out,i} e^{-j2\pi f \Delta} \quad (3.6)$$

Incorporating the delay equation into the simple transfer function, yields equation 3.7.

This is the complete transfer function for the circuit.

$$V_{out} = V_{in} \cdot \left(\frac{-\frac{R_2}{R_1}}{1 + j\omega R_2 C e^{-j2\pi f \Delta}} \right) + Er \cdot \left(\frac{j\omega R_2 C e^{-j2\pi f \Delta}}{1 + j\omega R_2 C e^{-j2\pi f \Delta}} \right) \quad (3.7)$$

3.2.2 DSM Pump Control

The incorporation of DSM control of the pump replaces other methods of pump control with the DSM methodology. A block diagram of the DSM controlled charge pump is shown in Figure 25.

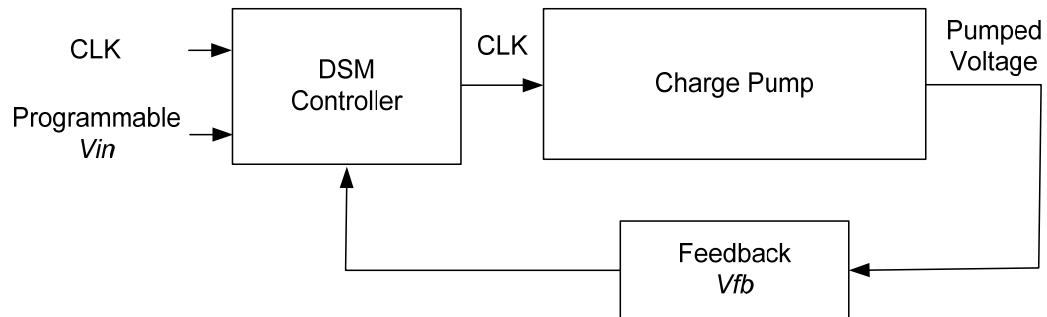


Figure 25. DSM Controlled Charge Pump

The programmed value of V_{in} is determined by the controlling algorithm and is used as the controlling voltage for the DSM pump controller. The DSM controller determines when the clock signal is fed to the charge pump based on the difference between the V_{in} value and the feedback pumped voltage, V_{fb} . The inputs to the DSM controller are the same as prior pump controllers. The V_{in} signal, which determines the set point of the DSM controller and CLK , drives the voltage pump.

3.2.3 Developing the Delta signal

The first stage of the DSM controller is circuitry necessary to develop the Delta signal. This is done through a switched capacitor matrix, Figure 26. The inputs to this circuit are the programming voltage, V_{in} , the fed back voltage from the charge pump, V_{fb} and the two non-overlapping clock signals CLK and CLK^* .

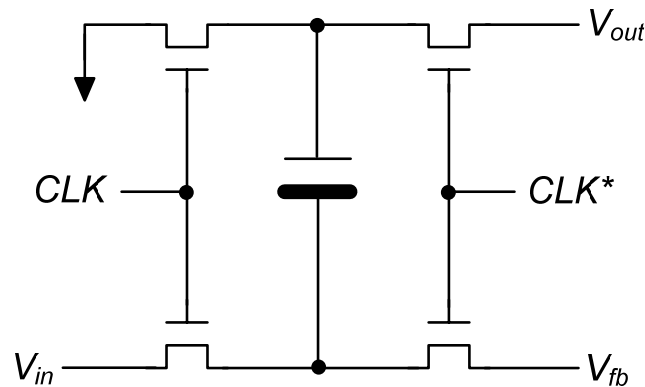


Figure 26. Switched Capacitor Circuit (Delta)

The output of this circuit is the signal V_{out} . This is the signal fed to the amplifier in the Sigma stage.

3.2.4 Developing the Sigma signal

The function of the Sigma integrator is to accumulate, or sum, the difference between V_{in} and V_{out} . The schematic in Figure 27 shows that the two inputs to the integrator are ground and the output signal from the switched capacitor stage. As this value is integrated over time an analog difference signal is generated that represents the difference between V_{in} and V_{out} . When the V_{in} is greater than V_{out} the integrator drives the positive output of the integrator more positive and the negative output more negative. This difference enables the clock signal to the charge pump. As the cumulative difference between V_{in} and V_{out} decreases, the input to the integrator is gradually driven to ground. Once the two levels are equal the outputs of the integrator switch relative polarities, the positive output is below the negative output. This disables the charge pump.

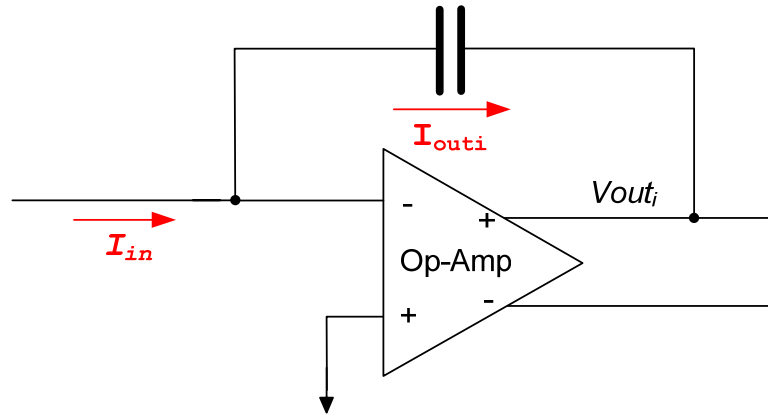


Figure 27. Integrating Amplifier, Sigma stage

3.2.5 Connecting Delta to Sigma

The circuit diagram in Figure 28 shows how the Delta and Sigma portions of the circuit are connected together. The output node of the Delta circuit, V_{out} , is connected to the inverting input to the differential amplifier. The reference node is connected to ground in both the Delta circuit and the Sigma circuits. The input value, V_{in} , is compared to V_{fb} and then this difference is integrated, averaged, by the integrating amplifier. The results of this integration control whether or not the pump is enabled.

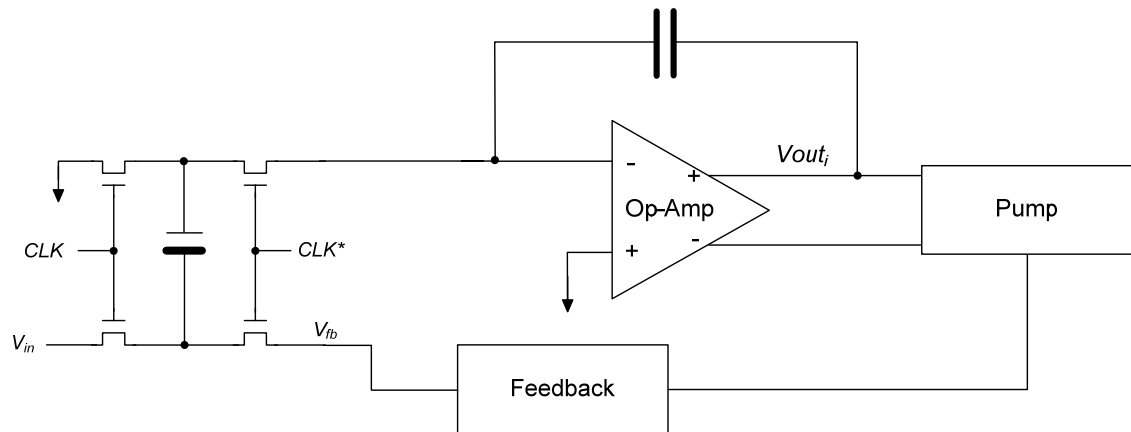


Figure 28. Complete Delta-Sigma Circuit

3.2.6 Delta-Sigma Operation

In order to show how the DSM can be used to control the pump the pump will be started with an initial condition that pump is idle V_{out} and V_{in} are at 0 V and CLK is not running. The CLK is started and allowed to stabilize. V_{in} is applied to the input of the DSM circuit. Since V_{in} is greater than V_{fb} there will a difference in the magnitude of the charge on the capacitor. The Q_{in} value, $(V_{in} * C)$ will be greater than the fed back charge value, Q_{fb} , $(V_{fb} * C)$. This will cause the current to flow from the node connected to the op-amp in order to balance the charge. This node will decrease and the op-amp will attempt to compensate for the input imbalance it sees and drive the V_{out} signal higher. This will enable the charge pump. Figure 29 illustrates this condition.

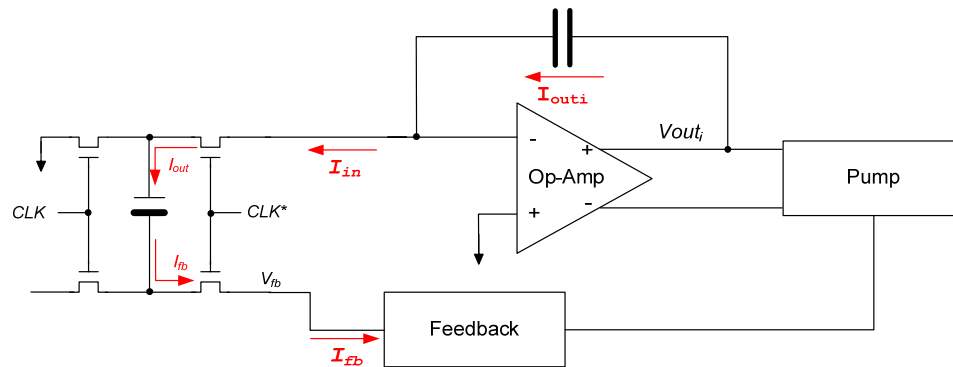


Figure 29. Current path when V_{in} is greater than V_{fb}

As the charge pump operates the V_{fb} value will increase and the difference between Q_{in} and Q_{fb} will decrease. Once the pump has operated long enough the V_{fb} value and the V_{in} value will be equal. When this condition is achieved the charge that is placed on the capacitor, Q_{in} , will equal the charge that is placed on it from the V_{fb} signal,

Q_{fb} . As a result there will be no charge flow from the output node. This will cause the DSM to turn off the enable signal to the pump.

Since there is a delay in the pumps response to the turn off signal from the DSM the output level, V_{fb} , will rise above the input signal, V_{in} . In this case the charge Q_{in} will be less than the feedback charge, Q_{fb} . As illustrated in Figure 30 this will cause a reversal of the current flow and the output level, V_{out} , will increase.

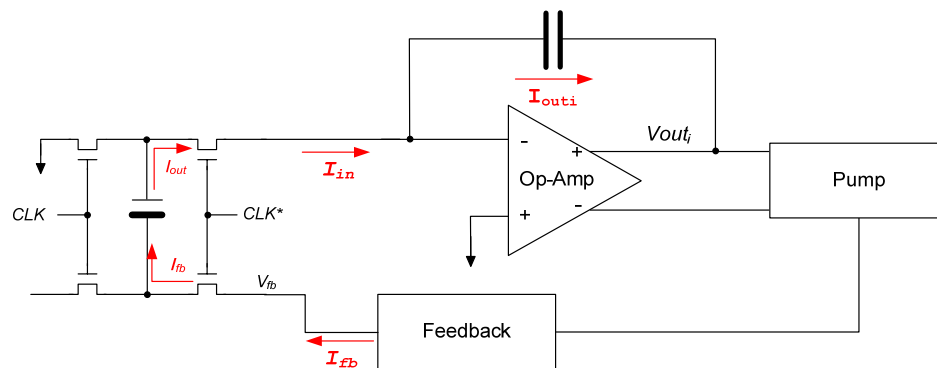


Figure 30. Current path when V_{in} is less than V_{fb}

3.2.7 Complete Circuit

The entire circuit is shown in Figure 31. In the complete schematic there is a clocked comparator in the forward path and an additional amplifier in the feedback path. The clocked comparator receives the bit stream from the Sigma stage and amplifies the output from the integrating amplifier and delivers the Enable signal to the pump. The feedback network schematic is shown in Figure 32. The resistors produce the required 10:1 voltage ratio and the unity gain amplifier isolates the Delta circuit from the output.

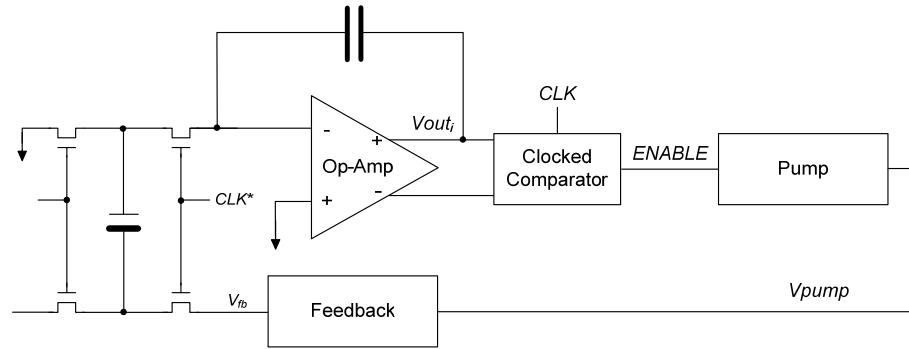


Figure 31. Completed Schematic of DSM controlled High Voltage Pump

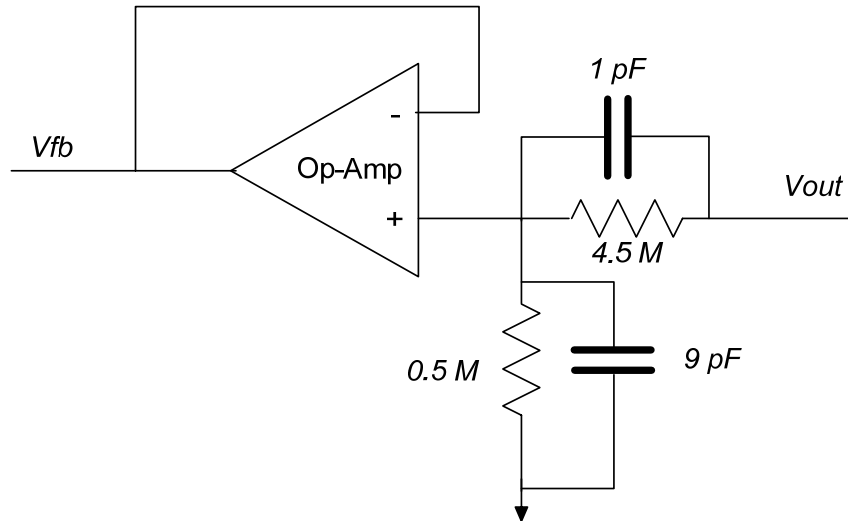


Figure 32. Feedback network schematic

CHAPTER FOUR: CHIP TEST RESULTS

4.1 Simulation and Experimental Methodology

The DSM controlled high voltage charge pump was designed and fabricated using AMI's 500 nm process through the MOSIS service. Characterization of the DSM controller to transient as well as DC operating conditions was conducted. Measurements included determining the range of appropriate V_{in} values, controller sensitivity to changes in V_{in} as well as a how fast the controller responds to a change in V_{in} . The controller was also characterized to determine its response to a change in the V_{pump} signal to determine the feedback path delay.

The floor plan of the chip is shown in Figure 33. The DSM controlled charge pump is laid out across the bottom of the die and each circuit component was placed around the remaining sides. The placement of the individual circuit components around the chip is for testing purposes and serve as a backup should the fully integrated circuit have not performed.

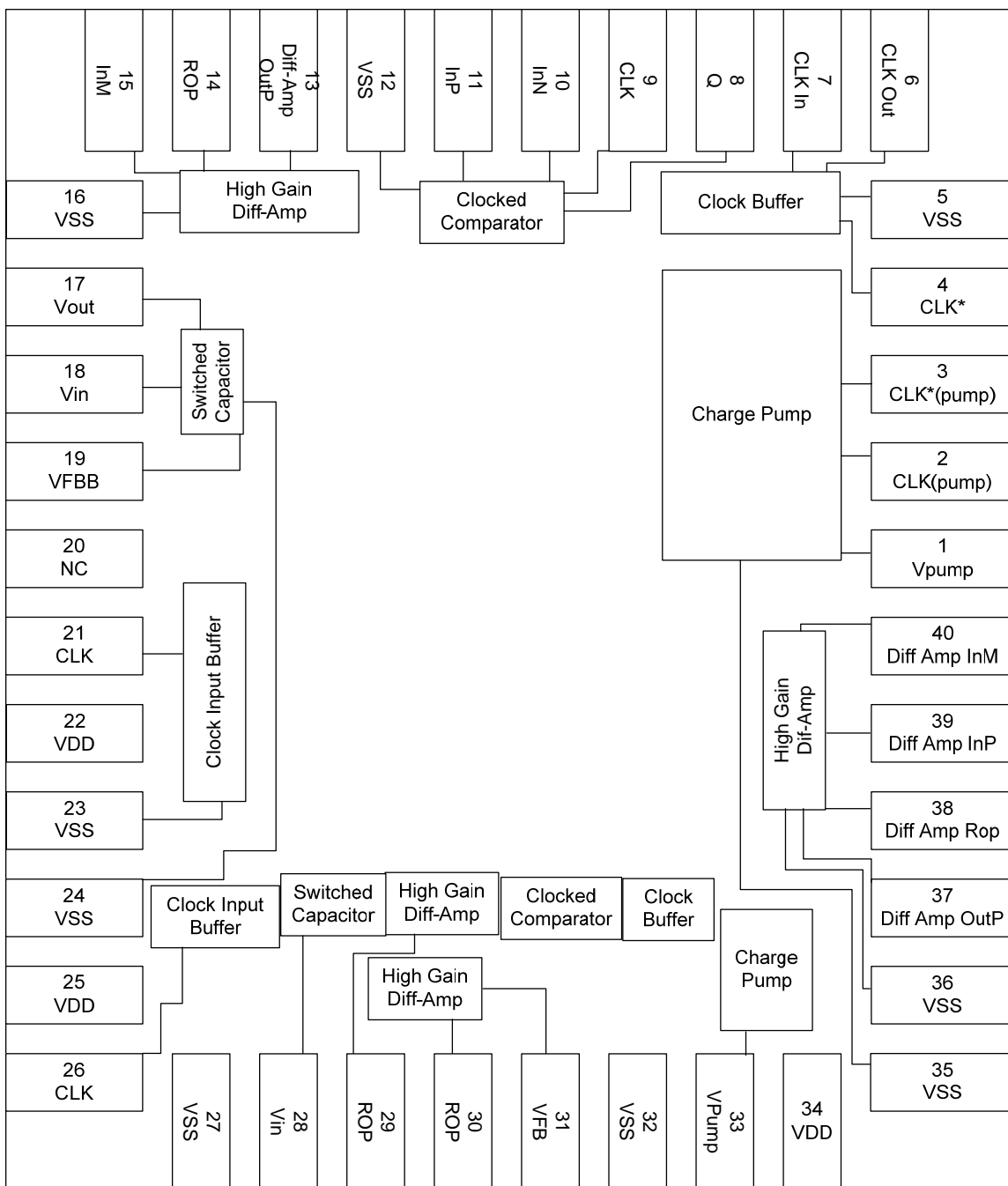


Figure 33. Die floor plan and pin assignment

Figure 34 shows the photograph of the chip after manufacture. The complete DSM controlled charge pump is located on the bottom of the chip and the individual

circuits can be seen around the remaining sides. The wired bonds can be seen lining the periphery of the chip with pin one as the center bond pad on the right hand side.

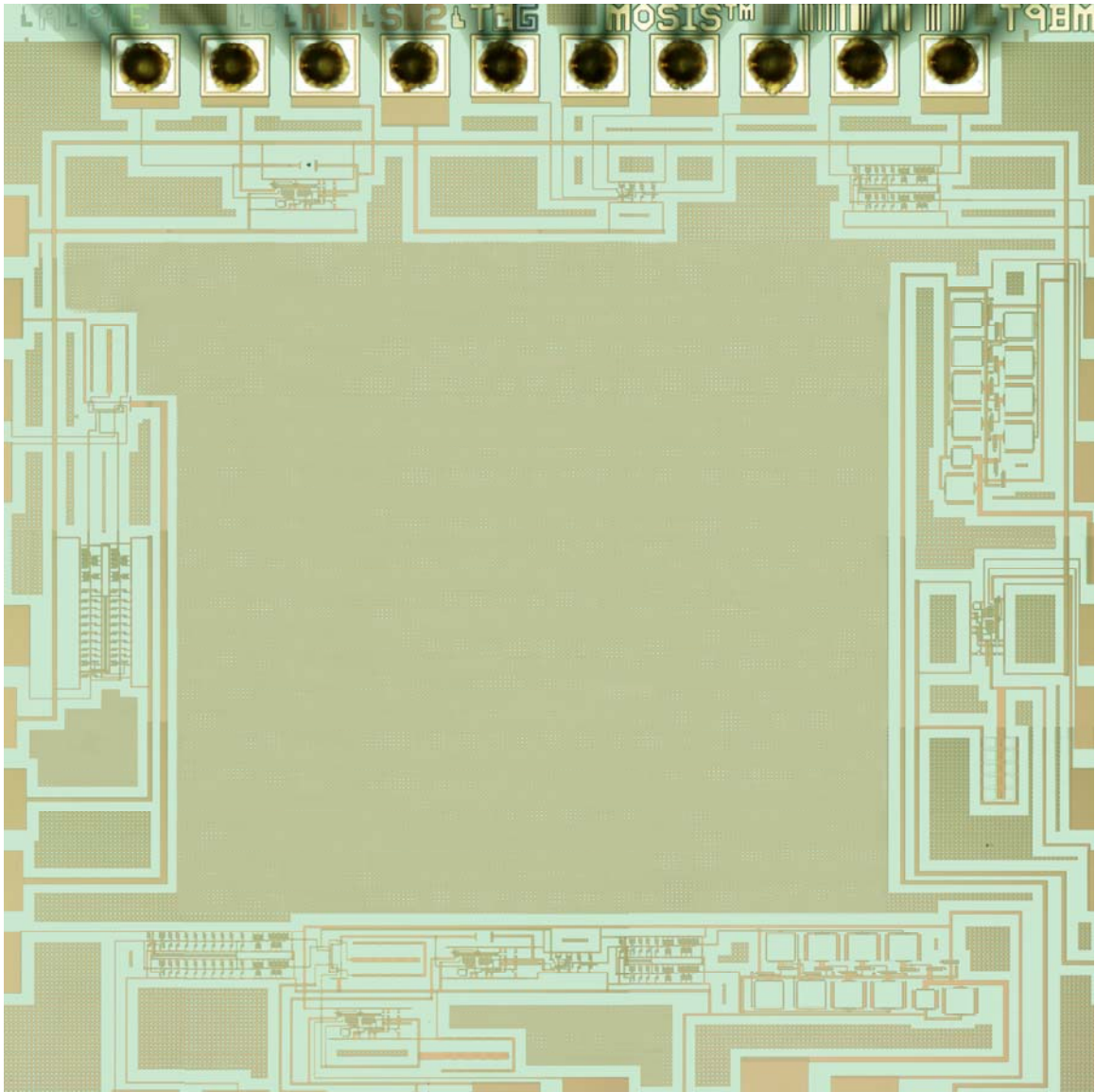


Figure 34. Chip photograph

Table 2 shows the pin assignments for the circuit elements on the chip. Note that each major circuit component has an individual Vss connection. This is to allow for separating each circuit should it be necessary due to a manufacturing or design flaw in the chip.

Table 2. Package Pin Assignments

Pin	Function	Pin	Function
1	Vpump (pump)	21	CLK in (CLK Input Buffer)
2	CLK (pump)	22	VDD
3	CLK* (pump)	23	VSS(CLK Input Buffer)
4	CLK* (CLK Buffer)	24	VSS (Switched Cap)
5	VSS (CLK Buffer)	25	VDD
6	CLK (CLK Buffer)	26	CLK (DSM)
7	CLK in (CLK Buffer)	27	VSS
8	Q (Clocked Comparator)	28	Vin (DSM)
9	CLK in (Clocked Comparator)	29	ROP (DSM)
10	In N (Clocked Comparator)	30	ROP(DSM)
11	In P (Clocked Comparator)	31	VFB (DSM)
12	VSS (Clocked Comparator)	32	VSS
13	Out P (Diff-Amp)	33	Vpump (DSM)
14	ROP (Diff-Amp)	34	VDD
15	IN M (Diff-Amp)	35	VSS (Charge Pump)
16	VSS (Diff-Amp)	36	VSS (Diff-Amp)
17	Vout (Switched Cap)	37	Out P (Diff-Amp)
18	Vin (Switched Cap)	38	ROP(Diff-Amp)
19	VFBB (Switched Cap)	39	In P (Diff-Amp)
20	NC	40	In M (Diff-Amp)

Figure 35 shows the characterization bench for the chip. A function generator was used to provide the 15 MHz clock signal and a power supply was used to provide the programmed input voltage, V_{in} . The output was measured with an oscilloscope and a digital volt meter.

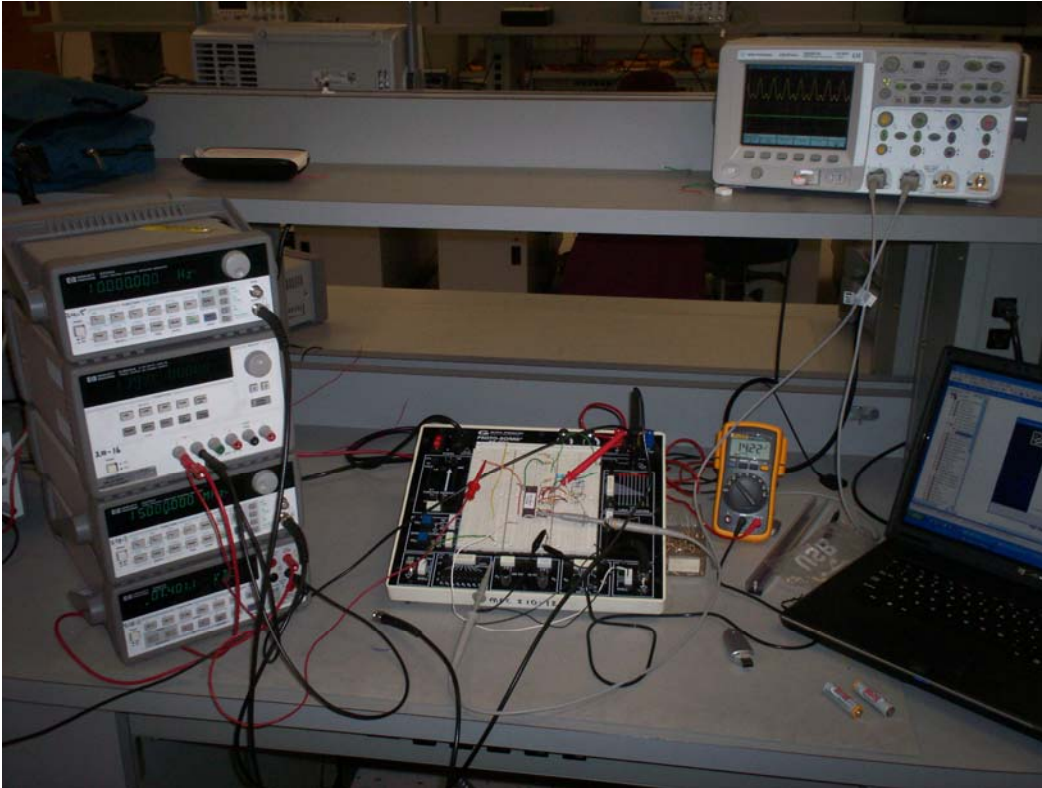


Figure 35. Characterization bench setup

4.1.1 Charge pump testing

A Dickson Charge pump [6], [8] was used to test the response of the DSM controller on an actual charge pump. The open loop response of the pump was simulated to reach 36 V with no load. The pump can maintain 20 V with a DC load of 50 μa with a load capacitance of 5 pF. The layout of the charge pump is shown in Figure 36.

The charge pump performance was tested and the results closely match the simulation results. The open loop response of the pump measured 38 V and the loaded voltage measured 19 V. Figure 37 shows the photograph of the charge pump in the fabricated chip.

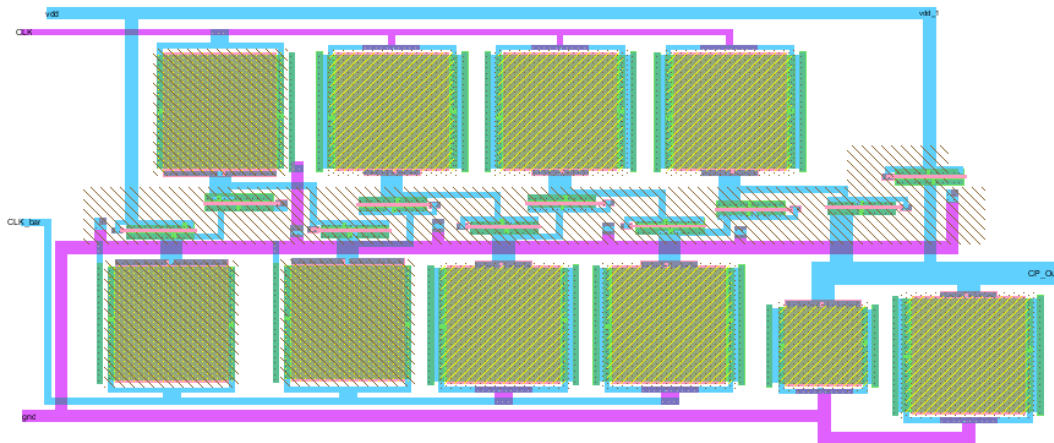


Figure 30. Charge pump layout

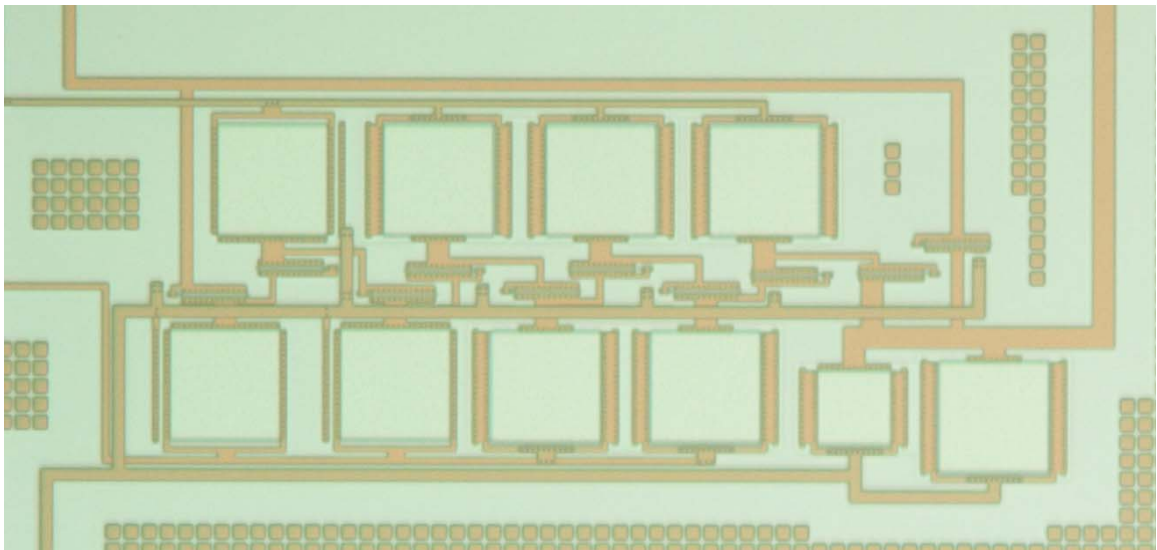


Figure 37. Charge pump photograph

4.1.2 Transient response analysis

The transient response of the circuit was measured using two different methods. The first transient response measured the startup response with different V_{in} values. The circuit was started up and V_{in} values ranging from 0.6 V to 2.0 V were applied to the

input. Once the V_{in} value was set the DSM response time was measured. Simulation data showed that the DSM circuit would have an initial response of 102 ns, two clock periods, at startup with the range of V_{in} values from 0.7 V to 2.0 V. The startup value for the 0.6 V, V_{in} , value was slightly slower at 152 ns, three clock periods. When V_{in} was increased to 1.75 V the response time decreased to 50 ns, one clock period. This response indicates the speed at which the DSM controller can respond to the programmed voltage, V_{in} , changing to meet the demands of the NAND controller. Figure 38 shows the response to a change in V_{in} from 0 V to 0.75 V. The DSM sensing circuitry senses the change and begins to clock the charge pump within in 100 ns.

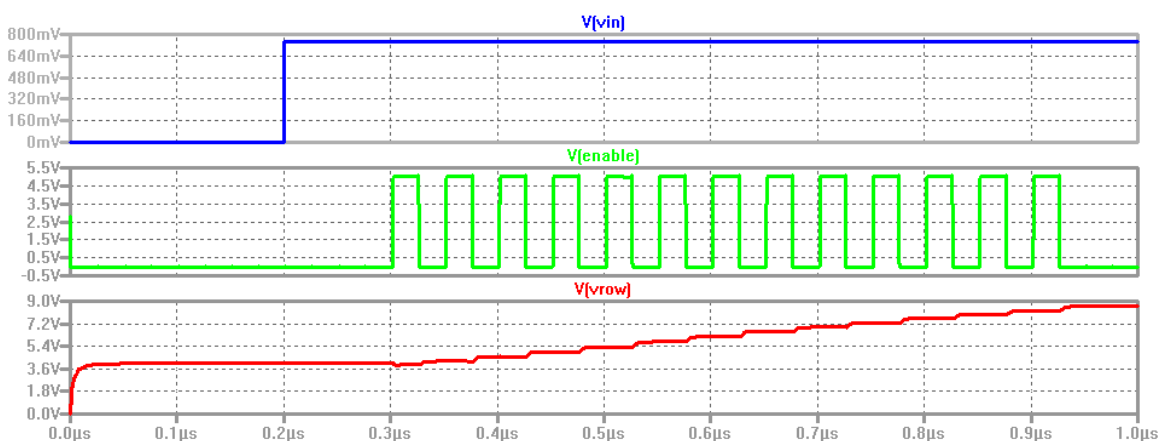


Figure 38. DSM response to V_{in} level change 0 V to 0.75 V

The V_{in} signal, blue, transitions from 0 V to 0.75 V at 200 ns. At 300 ns the pump signal is initiated to the charge pump and the output, V_{row} , red, begins to rise. At the 1 μ s interval the charge pump has elevated the output to the desired level. 0.78 V, and the charge pump has stopped pumping the output.

The response time of the DSM control circuit to a level adjustment of V_{in} was also characterized. The circuit was initialized to a V_{in} level of 0.75 V and then after stabilization the V_{in} level was increased to 2.0 V in 0.25 V increments. A plot of the data, Figure 39, shows that the DSM controller has a fast response time, less than 4 clock periods, to changes in the programmed input voltage. As the set point change magnitude increases above 1 V the response time settles at a minimum value of one clock period. Both simulated and measured data was taken with a clock period of 66 ns as the frequency generator used in testing was limited to 15 MHz.

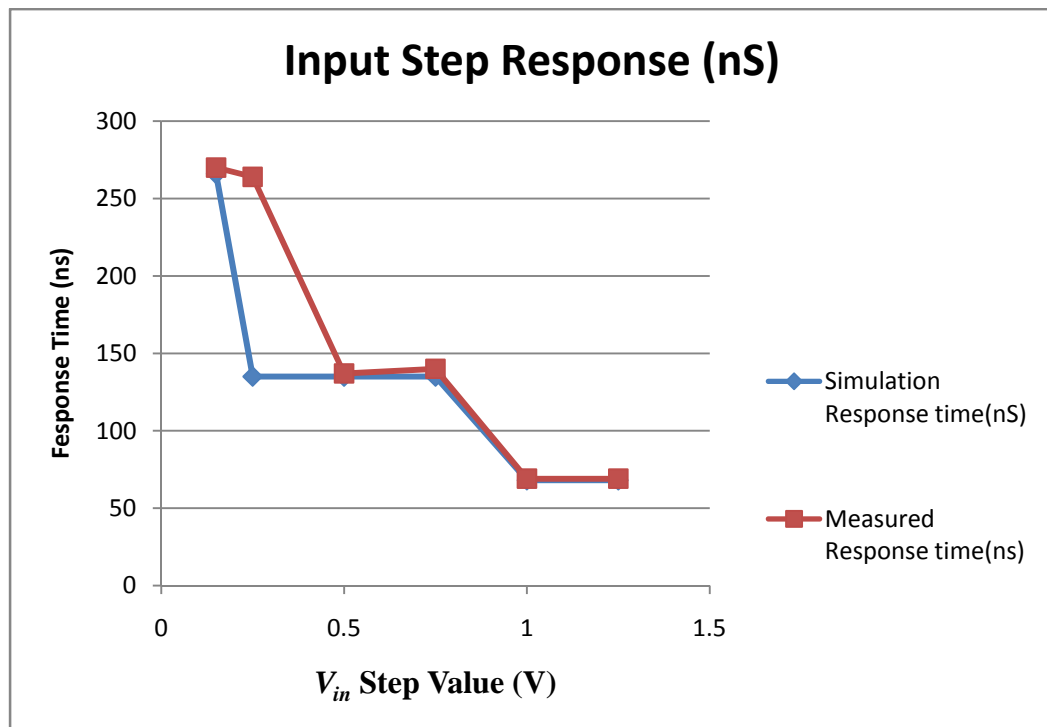


Figure 39. Response time to start up

The response of the DSM controller to the output reaching a desired set point and then responding to a load change was also tested and simulated. The simulation results in Figure 40 shows that the response time to the output reaching the programmed level is

190 ns and the DSM response to the output dropping below the desired set point is 108 ns. In this simulation the DSM circuitry was started and the programmed input voltage, V_{in} , light green, ramped from 0 V to 1 V at $0.2 \mu\text{s}$. This was sensed by the DSM controller at $0.32 \mu\text{s}$ as indicated by the V_{enable} , blue, signal initiating the clock to the charge pump.

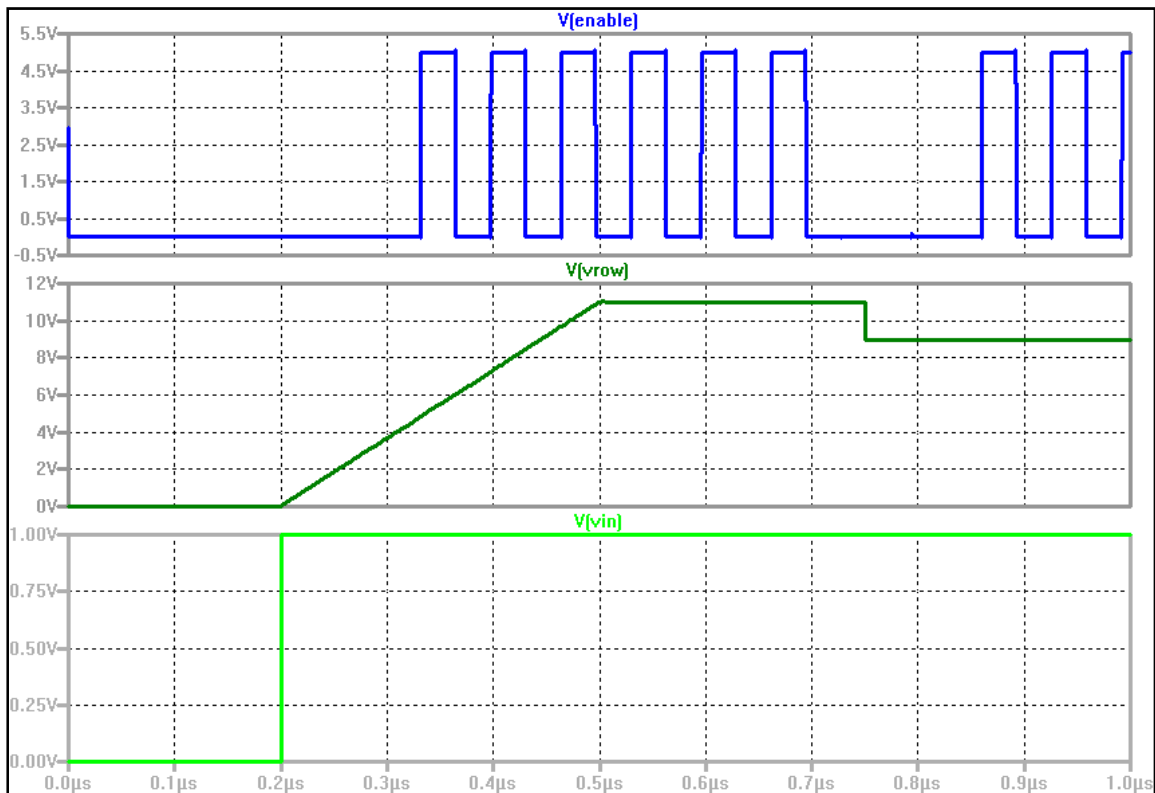


Figure 40. DSM controller response to varying output conditions.

The V_{row} signal was then ramped in SPICE simulating the charge pump output ramping to the desired level. At the $0.75 \mu\text{s}$ point the V_{row} signal was decreased below the set point determined by the V_{in} level. The DSM sensed the output and enabled the clock signal to the charge pump within $105 \mu\text{s}$, indicated by the V_{enable} signal toggling again.

During testing of the chip the output was loaded with a programmable power supply once the output was at the programmed voltage. The results showed that the circuit would respond within two clock periods, 120 ns, in close agreement with the simulation data.

4.1.3 Delta V_{in} Sensitivity

The DSM controller was also characterized to determine the minimum step transition on V_{in} that could be detected by the circuit. The smallest change in V_{in} that the circuit can detect is 100 mV. This was simulated with a programmed V_{in} level at one set point and then after the pump had stabilized the V_{in} level was changed. Simulation data for this change shows that the 100 mV change was sufficient for the DSM to detect and enable the charge pump. Figure 41 shows the simulation of the V_{in} , blue, value changing from 0.75 V to 0.85 V. The DSM detects the 100 mV change and enables the charge pump, V_{enable} , green, within 200 ns. The output, V_{row} , red, also shows that the output is driving to the new programmed level. Experimental data agreed closely with the simulation. The charge pump output would begin rising, within 250 ns, four clock periods.

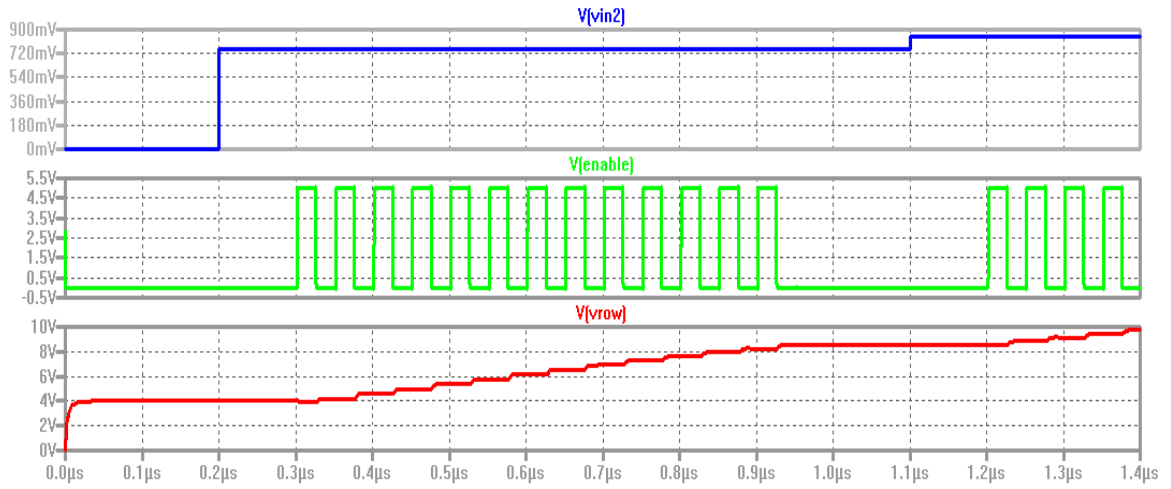


Figure 41. DSM detecting a V_{in} change of 100 mV

4.1.4 Linearity

The linearity of the pump is plotted in Figure 42. The desired set point was designed to have a 10:1 ratio of V_{out} to V_{in} . The simulation data shows good correlation to the ideal characteristic.

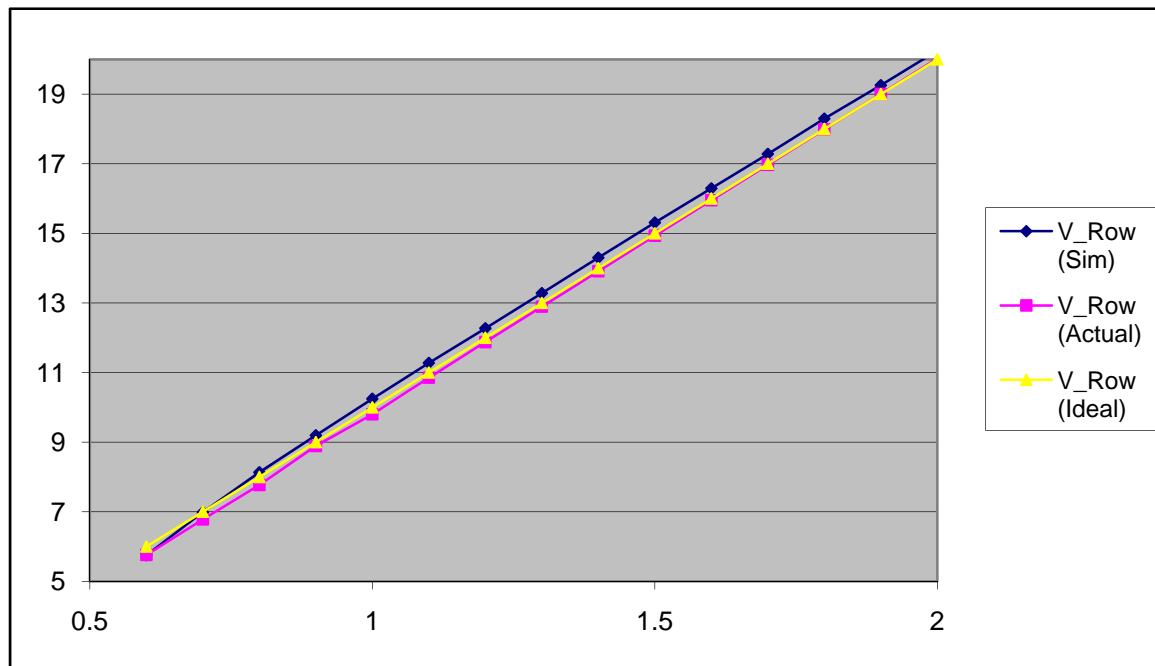


Figure 42. V_{out} Linearity with V_{in}

The average deviation in simulation is approximately -200 mV from the ideal. The measured response of the circuit is also plotted. The average variation or the measured values is 100 mV.

4.1.5 V_{out} ripple

The output ripple of the pumped voltage was simulated with different load capacitances. The pump is a simple 8 stage Dickson Charge pump [6], [8]. The simulated load capacitance was varied between 0.5 pF, 5 pF and 10pF as seen in Figure

43. The ripple voltage was measured with a 2.8 pF load capacitance and closely matched the simulation value for the 5 pF capacitance. This difference is most likely due to the affect of the test fixture capacitance on the overall load capacitance.

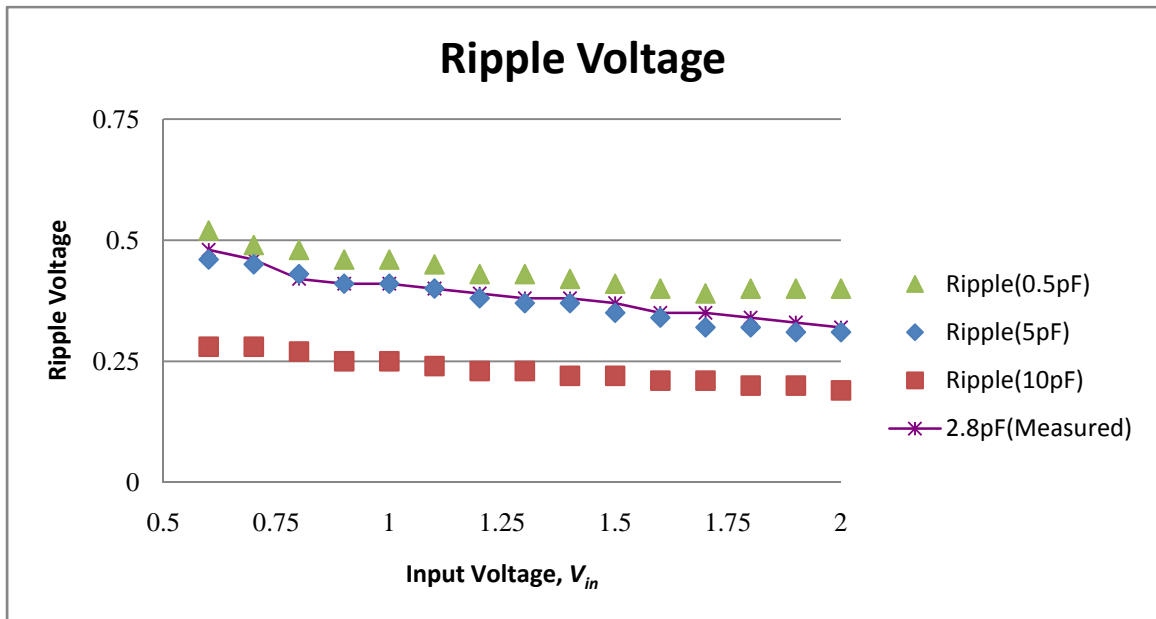


Figure 43. V_{out} Ripple with varying load capacitance

The ripple and the response time of the charge pump can be optimized with a more complex pump design, which is a topic for future research. It should be noted that the ripple can be reduced by reducing the size of the devices in the charge pump. The drawback of size reduction is that the amount of current the pump can supply also decreases.

The ripple on the output of the charge pump can be reduced with an increase in the load capacitance or the inclusion of a more complex pump circuit. The increase in load capacitance will decrease the ripple effects but will require an increase in layout area and a decrease in the pump response time. A more complex pump circuit could be use that incorporates different phases of the clock signal to pump the output at different

times. This method would effectively increase the frequency of the pump putting charge on the output capacitor. This would also require a more complex pump design and clock driver scheme, consume more area on the chip and increase the power consumption of the circuitry.

4.1.6 Summary

The design of a Delta Sigma modulation controller for a charge pump has been discussed. The design method was presented with special attention given to the advantages of the DSM method over other design methods as well as the performance of the DSM in the control of a charge pump. The DSM controller was fabricated using the AMI 0.5 μm process through the MOSIS fabrication organization and the chip performance was characterized and compared to simulation results.

CHAPTER FIVE: CONCLUSIONS AND FUTURE WORK

5.1 Conclusions

The design of a delta-sigma modulation controller for a charge pump is presented in this work. The DSM controller was designed to achieve a 100 mV resolution with a programmable input level. The controller had a gain factor of 10 so that low voltages could be used to control the higher voltage charge pump output. Special attention was given to the resolution and accuracy of the controller and the response time to changes in the input levels.

The DSM controller was chosen for its superior accuracy and resolution characteristics through the use of the averaging characteristics of the DSM methodology. The DSM controller was shown to have a high degree of sensitivity to the programming potential and a high degree of resolution in setting the output potential.

One of the limiting factors in this design is the delayed response of the DSM controller to the charge pump reaching the programmed potential. This delay in the pump response can be masked during normal NAND operations. One method would be to adjust the high voltage during the program verify operation. This would allow the high voltage to be ready, if necessary, to subsequent programming operations. This delay is primarily caused by the feedback network. The delay is determined by the RC delay of the voltage dividing resistors that sense the output voltage and feed this through to the

DSM controller. The DSM controller does have advantages over conventional methods of generating programmable potentials in greater sensitivity, noise immunity and sensitivity.

5.2 Future Work

Some areas of future exploration could improve the feedback path response time and increasing the programming range of the DSM controller. Also, in order to improve on the overall characteristics of the DSM a greater level of response to the programming input voltage, V_{in} , could be improved. This increase in sensitivity would allow for tighter placement of output levels and tighter programming ranges. The addition of a multi-phase charge pump on the controller would allow for a decrease in the ripple magnitude and develop a faster response to circuit demands.

The precision at which the threshold levels can be programmed in modern NAND devices could be greatly expanded in the programming voltages could be easily controlled. As the VDD levels of modern NAND devices are driven down in order to conserve power the programming range is also decreased. In addition to this requirement the drive to store more levels in each NAND location is being driven upwards. With these competing requirements the ability to accurately place the threshold of the device and the drive to place more thresholds in each device drive the need for methods to control the programming of each cell to higher degrees of accuracy. The DSM methodology can be used to improve the control of the charge pump and allow for greater resolution and accuracy in the placement of the programming voltages in the NAND cell.

Exact placement to within 10's of millivolts can be used to increase the capacity and decrease the overall voltage consumption of the device.

REFERENCES

- [1] Choi, Young, NAND Flash – The New Era of 4 bit per cell and Beyond, Semiconductor Insights, 2009
- [2] Takeuchi, Ken, et al, “A Source-Line programming Scheme for Low-Voltage Operation NAND Flash Memories,” IEEE Journal of Solid State Circuits, vol 35, no 5, pp 672 – 681, May 2000.
- [3] Tanzawa, Toru, et al, “Circuit Techniques for a 1.8V-Only NAND Flash Memory,” IEEE Journal of Solid State Circuits, vol. 37, no. 1, pp 84 - 89, January, 2002.
- [4] Hu, Chung-You, “Bias Scheme of Program Inhibit for Random Programming in a NAND Flash Memory,” USPTO, 1998, patent 5,715,194.
- [5] Kim, Jin-KI, et al, “Low Stress Program and Single Wordline Erase Schemes for NAND Flash Memory,” pp 19-20, MOSAID Technologies, 2007.
- [6] Pylarinos, Louie, “Charge Pumps: An Overview,” University of Toronto.
<http://citeseerx.ist.psu.edu/viewdoc/download?doi=10.1.1.128.4085&rep=rep1&type=pdf>
- [7] Baker, R. Jacob, CMOS, Circuit Design, Layout and Simulation, Revised 2nd Ed., IEEE Press, 2008, ISBN 978-0-470-22941-5.
- [8] Baker, R. Jacob, Keeth, Brent, DRAM Circuit Design, A Tutorial, IEEE Press, 2001, ISBN 0-7803-6014-1.
- [9] Suh, Kang-Deog, et al, “A 3.3V 32Mbb NAND Flash Memory with Incremental Step Pulse Programming Scheme”, IEEE Journal of Solid State Circuits, vol. 30, no. 11, pp 1149 - 1156, November, 1995.
- [10] Park, Ki-Tae, et al “A 64 Cell NAND Flash Memory with Asymmetric S/D Structure for sub-40nm Technology and Beyond,” 2006 Symposium on VLSI Technology Digest of Technical Papers, IEEE, 2006.
- [11] Micron Technology, Technical Note; Small-Block vs. Large Block NAND Flash Devices, 2007. <http://download.micron.com/pdf/technotes/nand/tn2907.pdf>
- [12] Shibata et al., "A 70-nm 16-Gbit 16-level-cell NAND Flash Memory," 2007 Symposium on VLSI Circuits, pp. 190-191.